ISSN 0719-045X

Clínica Alemana

Contacto Científico

Revista electrónica científica
y académica de Clínica Alemana

Especial Abstracts

SEGUNDA PARTE

2018

Contacto Científico

Revista electrónica científica y académica de Clínica Alemana.
Publicación bimensual

Misión

"Ser el medio oficial de difusión científico y académico de Clínica Alemana para la comunicación e intercambio de conocimientos, avances científicos y tecnológicos, con el fin de incrementar las competencias, habilidades, capacidades y todo aquello que mejore el cuidado de salud de las personas y contribuya al desarrollo del conocimiento médico en beneficio de la comunidad".

Conflictos de interés y responsabilidades

El Editor en Jefe y miembros del Comité Editorial, declaran no tener conflictos de interés o soporte financiero de empresas relacionadas.

Los editores de esta publicación, harán todos los esfuerzos para evitar errores e imprecisiones en las opiniones, declaraciones, cifras y datos publicados en esta revista. Sin embargo, los autores de cada uno de los artículos publicados son responsables del material enviado.

Los trabajos publicados en esta revista, pueden contener opiniones personales de los autores, por lo que no busca constituirse en la única fuente o guía para buenas prácticas y/o para un tratamiento adecuado y seguro.

Por lo anterior, los editores y personas que participan en su revisión, edición y publicación, quedan exentos de toda responsabilidad por las consecuencias que pudiesen ocurrir, producto de imprecisiones o errores en cifras, datos u opiniones.

Contenidos de esta edición

37 **Breast ductal carcinoma in situ presenting as a mass - not as unusual as we think**
Eleonora Horvath, Javier Cacho, Carla Darrás Ismael, Claudio Silva, Marcela Gallegos, Miguel Ángel Pinochet, María Elisa Droguett, Eduardo Soto, Heriberto Wenzel.

38 **Enlightening the forgotten organ: PET-CT findings on thymic lesions**
Claudio Silva, Giancarlo Schiappacasse, Julia Alegria, Daniel Hasson.

44 **The prostate anatomy, a useful tool for clinical practice: assessed through augmented reality**
María Fernanda Tapia, Daniel Hasson, Andrés Labra Weitzler.

46 **ITMIG classification of mediastinal anatomy: exposure through augmented reality**
María Fernanda Tapia, Daniel Hasson, Julia Alegría.

51 **Role of ultrasound in management of indeterminate thyroid nodules (Bethesda lll and IV)**
Eleonora Horvath, Camila de la Barra, Guillermo Aguilera, Claudio Silva, Jeannie Slater, Velimir Skoknic, Sergio Majlis, M. Garcia, Paulina González.

52 **Breast Fibromatosis Imaging Patterns Mimicking Breast Carcinoma -» Emphasis on Young Women**
Eleonora Horvath, Mónica Rochels, Claudio Silva, Miguel Angel Pinochet, Cecilia Galleguillos, Flavia Pizzolon, Valentina Villalón, Marcela Uchida, Eduardo Soto.

53 **Ultrasonographic Diagnosis of Salivary Gland Atrophy after Radio-iodine Treatment for Papillary Thyroid Cancer**
Eleonora Horvath, Velimir Skoknic, Claudio Silva, Hernán Tala, Nicolás Sánchez, Carolina Whittle, Juan Pablo Niedmann, Sergio Majlis, C. Schweinitz.

54 **Background parenchymal enhancement at breast magnetic resonance imaging - Association with tumor response to neoadjuvant chemotherapy**
Eleonora Horvath, Eliette Castillo, Claudio Silva, Carla Darrás, María Elisa Droguett, Cecilia Galleguillos.

55 **Can a hyperechogenic breast lesion be malignant?**
Eleonora Horvath, Eliette Castillo, Flavia Pizzolon, Claudio Silva, Marcela Gallegos, Miguel Angel Pinochet, Cecilia Galleguillos, Marcela Uchida, Paulina Gonzalez.

56 **Kikuchi-Fujimoto disease: report of 5 cases mimicking malignancy in axillary lymph nodes**
Eleonora Horvath, Sebastián Villarreal, Claudio Silva, Cecilia Galleguillos, Miguel Angel Pinochet, Valentina Villalón, Marcela Uchida, Heriberto Wenzel, Eduardo Soto.

57 **Prospective evaluation of extent of disease in prostate cancer biochemical relapse by [68Ga]PSMA-HBED-CC PET/CT**
Guillermo Chong, Daniela Barahona, Andrea Balcells, Daniel Hasson, Giancarlo Schiappacasse, Andrés Labra Weitzler.

58 **Atypical ultrasonographic patterns of papillary thyroid carcinoma: how to recognize them?**
Eleonora Horvath, Guillermo Aguilera, Claudio Silva, María Elisa Droguett, Velimir Skoknic, Hernán Tala, Sergio Majlis, Jeannie Slater, Carolina Whittle.

59 **Contribution of pre operative breast MRI study in pure DCIS**
Eleonora Horvath, Carla Darrás Ismael, Claudio Silva, Eliette Castillo, Miguel Angel Pinochet, Cecilia Galleguillos, María Elisa Droguett, Valentina Villalón, Flavia Pizzolon.

60 **Concordance and inter-reader agreement for PIRADS v2.0 in bi-parametric versus multi-parametric prostate MRI approaches**
Andrés Labra, Giancarlo Schiappacasse, Daniela Barahona, Claudio Silva.

61 **Abdominal pain: when the abdomen does not speak, the chest screams**
Daniel Schneider, Fabián Villacrés, Julia Alegría, Claudio Silva.

Editorial
Alerta
Buenas Prácticas Clínicas
Cartas al Editor
Casos Clínicos
Campañas y Revisión
Contribución Original
Controversias
Cursos y Congresos
Estado del Arte
Etica Médica
Farmacología
Guías y Protocolos
Investigación
Lectura Crítica
Links- Videos
Medicina Traslacional
Metodología de la Investigación
Misceláneos
Noticias
Para su Paciente
Perlas
Publicaciones CAS-UDD
Quiz
Revisión Clínica
Temas
Tips para Publicar
Trabajos Originales

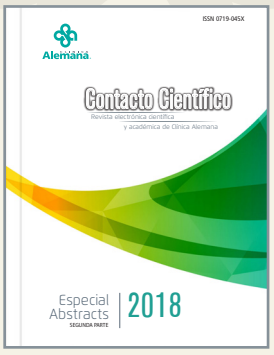

Contenidos de esta edición

63 **Three cases of Skene's gland cyst at pediatrics age**
Andrea Pichott Fontalba, Andrés Retamal Caro, Javiera Aguirre Fernández, Lizbet Perez-Marrero, Isabel Fuentealba Tapia.

64 **Vascular lymphatic malformations in paediatrics: Radiologic findings**
Javiera Aguirre Fernández, Andrea Pichott Fontalba, Lizbet Perez-Marrero, Isabel Fuentealba Tapia, Carolina Whittle.

65 **Appendicular lymphoid hyperplasia, differential diagnosis of acute appendicitis: Ultrasound findings**
Carolina Whittle, Lizbet Perez-Marrero, Marcela Cortés, Margarita Switt, Javiera Aguirre Fernández.

66 **Current hepatitis A outbreaks in men who have sex with men - Epidemiological situation in HIV patients in Chile**
Claudia Cortés, Marcelo Wolff, Luis Miguel Noriega, Alejandra Marcotti, Carla Palavecino, Pía Mateluna, Lorena Porte, Thomas Weitzel.

67 **Validation of a model predicting graft survival after liver transplantation: The Donor risk index (DRI) a useful tool in Latin America.**
Rodrigo Zapata, Alexandra Ginesta, Monserrat Rius, Fernando Gómez, Edgar Sanhueza, Jorge Contreras, Roberto Humeres, Guillermo Rencoret, Marcelo Vivanco, José Manuel Palacios.

69 **A quality improvement initiative: the quest for zero Central Line-associated Bloodstream Infections (CLABSI) in hospitalized infants in a Neonatal Intensive Care Unit (NICU) in Chile**
Juan Carlos Muñoz, Beatriz Milet, Marcela Gómez, Antonieta Vicentelo, Marta Contreras, Marissa Garrido, Carolina Avila, Pablo Gaete, Marcial Osorio.

75 **Seis pacientes con trombosis de seno venoso en tratamiento con Dabigatran.**
Marianella Hernández, Patricia Araneda, Sergio Illanes.

76 **Experiencia de atención odontológica bajo anestesia general en pacientes odontopediátricos con y sin necesidades especiales en salud. Estudio retrospectivo.**
Ximena Muñoz, María Consuelo Fresno, Javier Martin.

77 **Risk for central metastasis on papillary thyroid cancer patients with suspicious lateral lymph nodes and non suspicious central LN on preoperative staging ultrasound (US)**
Ingrid Plass, Hernán Tala, Eleonora Horvath, Paulina González, Juan Pablo Niedmann, Carolina Whittle, Jeannie Slater, Felipe Capdeville, Arturo Madrid, Hugo Rojas, Ricardo Rossi, Fabio Valdés.

78 **Pentoxyphylline inhibits M1 polarization and favors M2 of murine macrophages treated with TLR4 agonist**
María Cecilia Montero, Julia Guerrero.

80 **Extracorporeal life support in critical ill immunocompromised adult patients**
René López, Rodrigo Pérez, Jerónimo Graf.

82 **VE/VCO_2 slope is increased in patients who fail the spontaneous breathing trial**
René López, Rodrigo Pérez, Iván Caviedes, Jerónimo Graf.

85 **South American scrub typhus: first case series from continental Chile**
Thomas Weitzel, Constanza Martínez-Valdebenito, Gerardo Acosta-Jamett, Ju Jiang, María Pilar Gambra, Teresa Bidart, Miguel Lagos, Allen L. Richards, Katia Abarca.

86 **Imaging study of pulmonary vein stenosis**
Julia Alegria, Claudio Silva, Guillermo Aguilera, Gerhard Franz Garrido.

87 **Intracranial Aneurysms Assessment: What the Radiologists Should Report**
Tomas Bernstein, Nicolás Sanchez, Paulo Zuñiga Bustos.

88 **Inter-observer agreement in the classification of perifissural nodules as lymphnodes on chest CT**
Juan Carlos Díaz, Claudio Silva, Javier Cacho, Julia Alegría, Cristóbal Ramos.

Abstract 11.

Breast ductal carcinoma in situ presenting as a mass - not as unusual as we think

Eleonora Horvath, Javier Cacho, Carla Darrás Ismael, Claudio Silva, Marcela Gallegos, Miguel Ángel Pinochet, María Elisa Droguett, Eduardo Soto, Heriberto Wenzel.

Clínica Alemana de Santiago/CL

Presentado en European Congress of Radiology, 28 febrero – 4 marzo 2018, Viena, Austria.

Abstract

Purpose: To describe the imaging and histopathologic characteristics of pure ductal carcinoma in situ (DCIS) of the breast that presents as a breast mass.

Methods and materials: IRB approved, retrospective review of mammography (Mx), ultrasound (US) and MARI images of puro DCIS cases who underwent surgery in a ¡single institution between 2015 and 2017. Those cases that presented as masses in any breast imaging modalities were selected. Radiological findings and histopathological features of the surgical sample were recorded.

Results: On a total of 467 operated breast cancers, 41 (8.7%) case of pure DCIS were identified and 11 of them (9%) appeared as masses on different images, with or without microcalcifications. Two cases (22.2%) were US only lesions. In US 6 (54.5%) presented as low-intermediate suspicion masses (Bl- RADS 4a and 4b). The most common MARI appearance was non-mass like enhancement in six cases (54.5%). Ten nodular pure DCIS (90.9%) had intermediate or high nuclear grade; 10 (90.9%) had necrosis, 4 (36.3%) of them were comedy type. 80% expressed estrogen receptors, 60% progesterone receptors, and 40% were Her2 positive. Microscopic analysis showed massive distention of the mammary ducts with neoplastic cells that coalesced giving a nodular appearance.

Conclusion: Pure DCIS presenting as a mass is a more common scenario than previously thought, representing 26.8% of cases in our series. Almost half of them were low-intermediate suspicion lesions in US. Coalesced mammary ducts distended by malignant cells are responsible for the macroscopic nodular appearance.

Abstract 12 .

Enlightening the forgotten organ: PET-CT findings on thymic lesions

Claudio Silva,
Giancarlo Schiappacasse,
Julia Alegria,
Daniel Hasson.

Clinica Alemana de Santiago, RM/CL

Presentado en European Congress of Radiology, 28 febrero – 4 marzo 2018, Viena, Austria.
DOI-Link:http://dx.doi.org/10.1594/ecr2018/C-1753

Learning objectives

1. Present the imaging findings of thymic pathology on PET-CT
2. Explain the added value of using PET-CT when evaluating thymic lesions
3. Discuss advantages and limitations of this technique, and how it can complement CT and MRI

Background

Thymic lesions are being diagnosed more frequently as imaging tests have become readily available. Most thymic lesions are asymptomatic, so incidental findings are frequent. PET-CT is used as part of most oncologic procedures planning, and there are specific aspects of this technique that are important to be known by radiologists regarding this kind of lesions.

Findings and procedure details

We have selected cases that enlighten the most important aspects of PET-CT thymus imaging and how it can contribute to inaccurate diagnosis or for treatment planning. Specifically, we present an overview of common thymic lesions and mimics of disease, with an emphasis on PET-CT imaging findings, while also briefly commenting CT and MRI findings. Cases presented include normal thymus, thymic hyperplasia, thymic cyst, invasive thymoma, thymic carcinoma, and lymphoma.

Normal appearance of thymus and variation with age

- The normal thymus is a triangular, bilobed organ residing in the anterior mediastinum.
- Can appear quadrilateral with convex borders on young patients.
- Mild to moderate 18F-FDG uptake on young patients. Undergoes fatty infiltration with age and progressively reduces 18-FDG uptake.

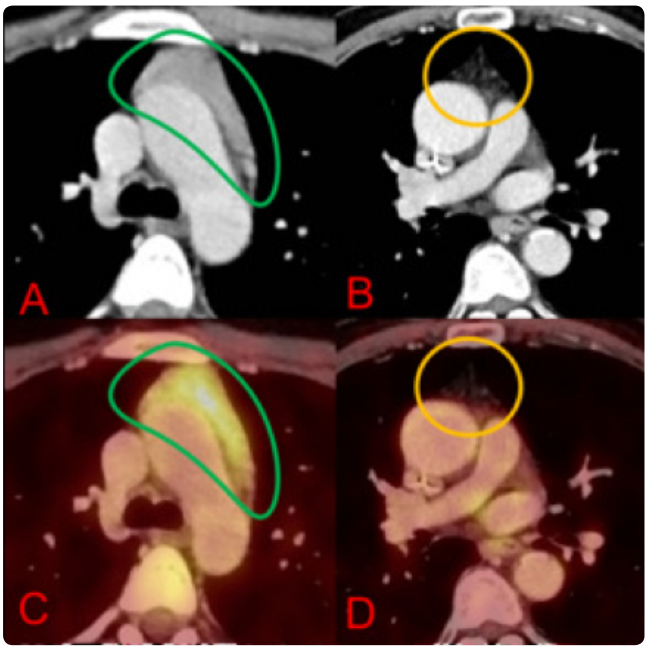

Figura 1.
Axial (A & B) CT chest and axial (C & D) PET-CT chest. 20-year-old (on the left) and 65-year-old (on the right) patients with no previous history of chemotherapy. The 20-year-old woman shows a quadrilateral thymus (green outline) with mild 18-FDG uptake (A & C), while the 65-year-old man shows a triangular thymus (orange outline) and no significant 18-FDG uptake (B & D).
References: Radiology Department, Facultad de Medicina UDD-CAS, Clinica Alemana de Santiago - Santiago/CL

Thymic hyperplasia

- Can be divided into true thymic hyperplasia and lymphoid hyperplasia (autoinmmune thymitis).
- Both entities present as diffuse symmetric thymus enlargement, so imaging cannot reliably distinguish them.
- True thymic hyperplasia appears posterior to stressful processes, such as chemotherapy, corticosteroid therapy, radiation therapy, burns or systemic infections.
- Lymphoid hyperplasia is associated to myasthenia gravis, systemic lupus erythematosus and Graves disease, among other autoimmune entities.
- Thymus usually losses its bilobed appearance and appears oval in CT and shows mild increase in 18F-FDG uptake.
- A triangle shape of 18F-FDG uptake is most frequent, but unilateral or midline patterns are possible as well.
- A SUVmax of less than 3.4 is suggestive of thymic hyperplasia, while over 3.4 is predictive of lymphoma.
- Chemical shift MRI can be useful for differentiating thymic hyperplasia from thymic tumors.

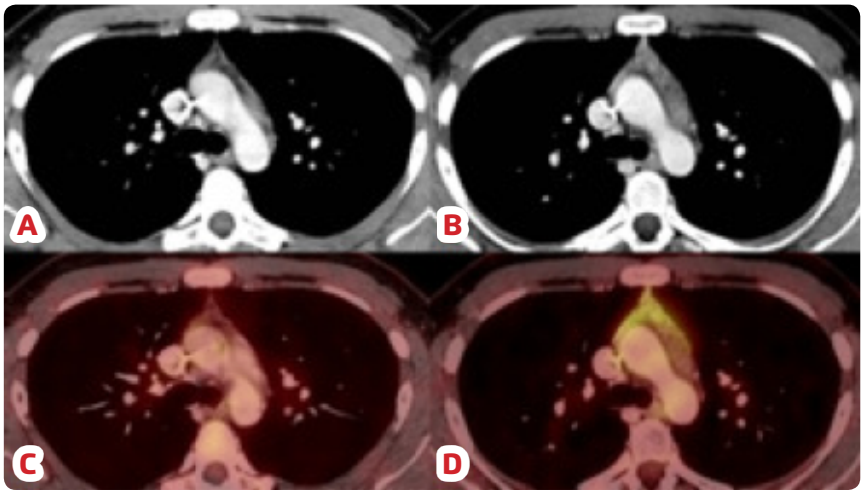

Figure 2.
Axial (A & B) CT chest and axial (C & D) PET-CT chest. A 21-year-old male underwent chemotherapy for testicular neoplasm. Pre– (A & C) and post– (B & D) chemotherapy 4 months apart images show a slight increase in thymus size and a midline-and-right-lobe pattern of 18-FDG uptake (SUV max: 3,8). A diagnosis of rebound thymic hyperplasia was made. The patient is doing fine after 2 years of follow-up.
References: Radiology Department, Facultad de Medicina UDD-CAS, Clinica Alemana de Santiago - Santiago/CL

Thymic cysts

- Can be divided into congenital cysts and adquired lesions. Secondary lesions can appear in relation to irradiated Hodgkin's lymphoma or in non-radiated thymic neoplasms such as thymoma or seminoma.
- Congenital cysts are unilocular lesions. Acquired thymic cysts are usually multilocular.
- Thymic cysts usually show fluid attenuation at CT but calcifications or hemorrhage are not uncommon findings.
- Thymic cysts do not normally exhibit significant 18F-FDG uptake.
- MR imaging can be used to differentiate hemorrhagic fluid from soft tissue.

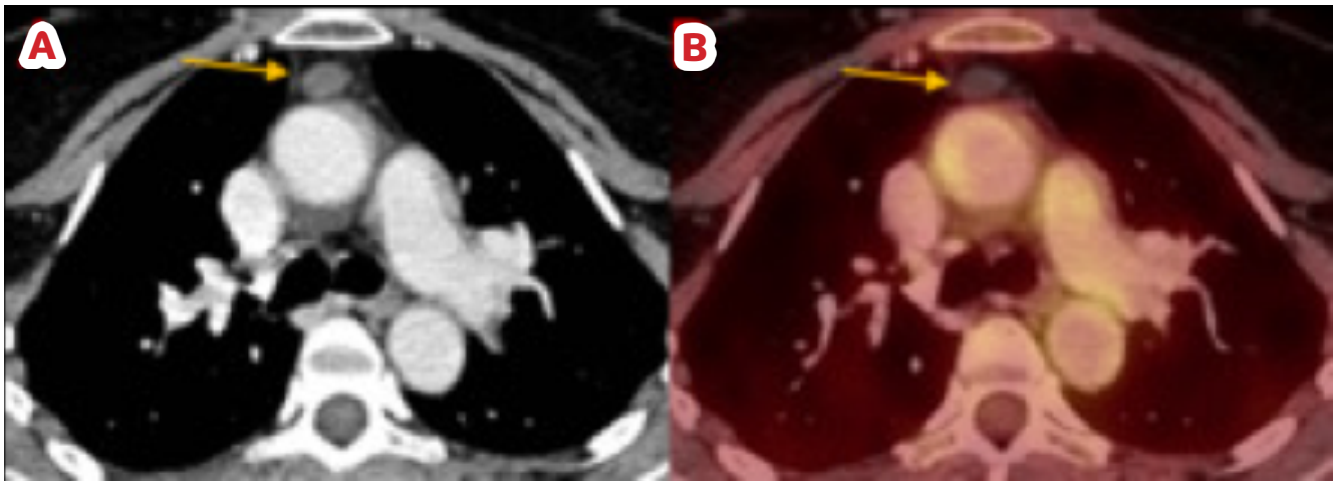

Figure 3.
Axial CT chest (A) and PET-CT chest (B). A 58-year-old female with an incidental finding of a simple appearing cyst in the region of the thymus (orange arrows); the lesion shows no significant contrast enhancement (CT density: 12 HU) nor 18F-FDG uptake. It has remained stable for 5 years and a diagnosis of thymic cyst was made.
References: Radiology Department, Facultad de Medicina UDD-CAS, Clinica Alemana de Santiago - Santiago/CL

Thymoma

- Thymomas are benign or low grade malignant tumors.
- Important association with myasthenia gravis.
- Calcifications are frequently seen in these lesions.
- Invasion of mediastinal structures, pleural thickening, or effusion are indicators of invasive tumor.
- Low-risk thymoma have a more heterogeneous uptake than high-risk thymoma.
- High-risk thymoma usually have a higher 18F-FDG uptake (SUVmax) than non-invasive thymomas, however, there is no definite SUV cut-off.

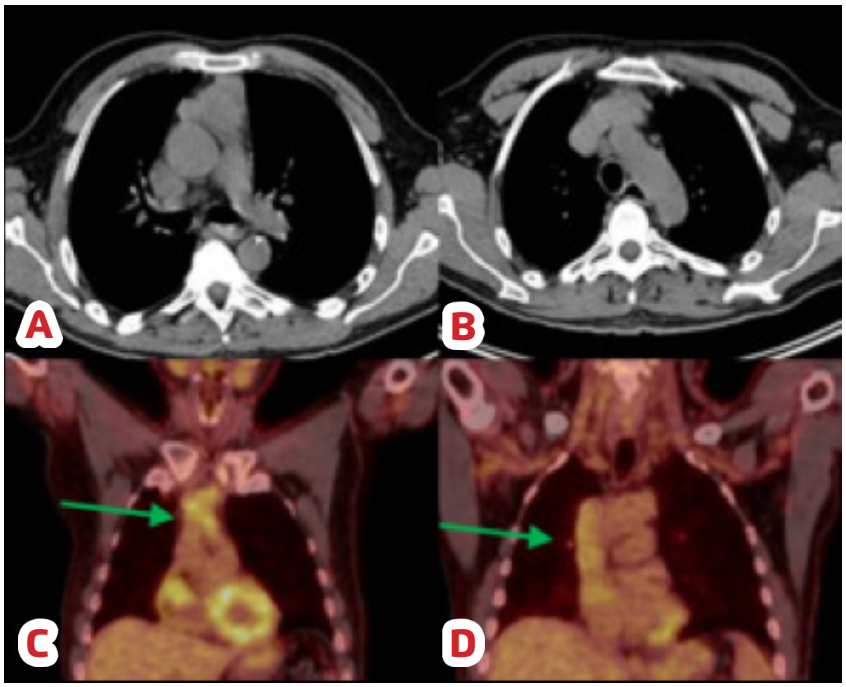

Figure 4.
Axial CT chest (A & B) and coronal (C & D) PET-CT chest. 52 year-old male. Prevascular mass with loss of a cleavage plane concerning for vascular invasion. PET-CT shows a hypermetabolic mass (SUV max 4.5) extending through the IVC into the right atria (green arrows). Surgery confirmed findings for an invasive thymoma.

Thymic carcinoma

- Thymic carcinomas are aggressive tumors with a high tendency for distant metastasis
- Usually present on CT as multilobulated heterogenous masses with areas of necrosis and calcification
- On 18F-FDG show high uptake. SUVmax is tipically over 7, which can help differentiate thymic carcinoma from thymoma.
- In addition, presence of mediastinal lymphadenopathy and distant metastasis on 18F-FDG PET-CT suggest thymic carcinoma

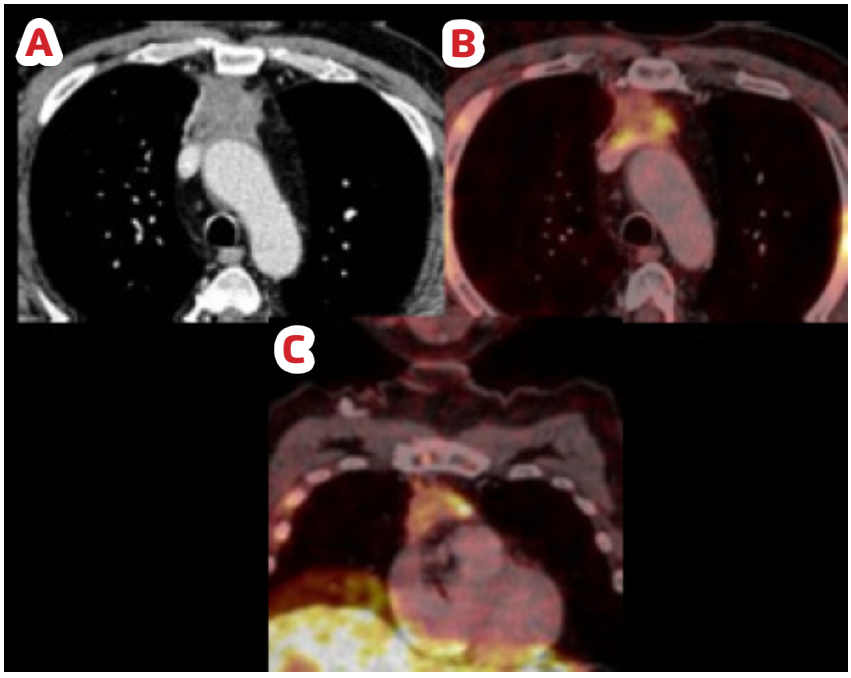

Figure 5.
Axial CT (A) and PET-CT (B) chest. Coronal PET-CT (C). Ill-defined prevascular (anterior) mass with heterogenous enhancement. PET-CT shows discrete areas of FDG uptake, yet highly metabolic at those points (SUV max 8.2). Pathology obtained at surgery revealed a thymic carcinoma.
References: Radiology Department, Facultad de Medicina UDD-CAS, Clinica Alemana de Santiago - Santiago/CL

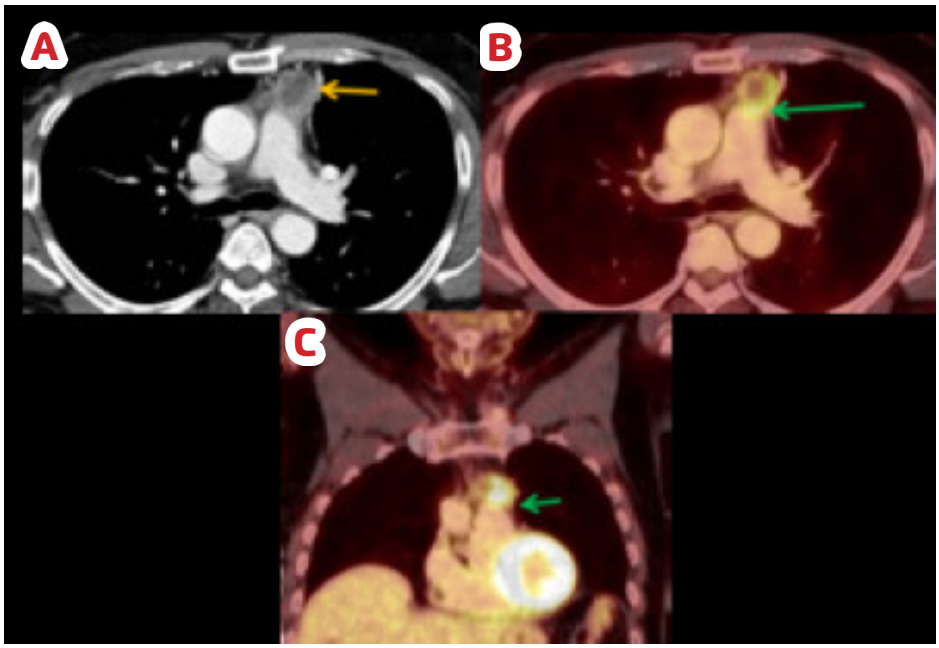

Figure 6.
Axial CT (A) and PET-CT (B) chest. Coronal PET-CT (C). 66-year-old male. Polilobulated prevascular mass with a solid peripheral contrast-enhancing component and a non-enhancing center compatible with necrotic center (orange arrow). High 18F-FDG uptake In the solid portion of the lesion (SUV max: 17.5). There is a loss of cleavage plane with the pulmonary artery on CT and PET-CT images (green arrows), as well as a subtle density of adipose tissue relative to the aortic arch, with no uptake increase. Pathology obtained at surgery revealed a thymic carcinoma.

Lymphoma

- Thymic involvement in lymphoma can occur in the setting of widespread disease or as isolated involvement.
- Hodgkin lymphoma is more frequent in this setting than non-Hodgkin's lymphoma
- PET-CT shows a nodular, usually asymmetrical thymus enlargement, with SUVmax usually over 3.4
- Higher 18F-FDG uptake is suggestive of more aggressive varieties: SUVmax values over 13 are highly suggestive of aggressive lymphoma, and less than 6 are associated with a high probability of indolent lymphoma.

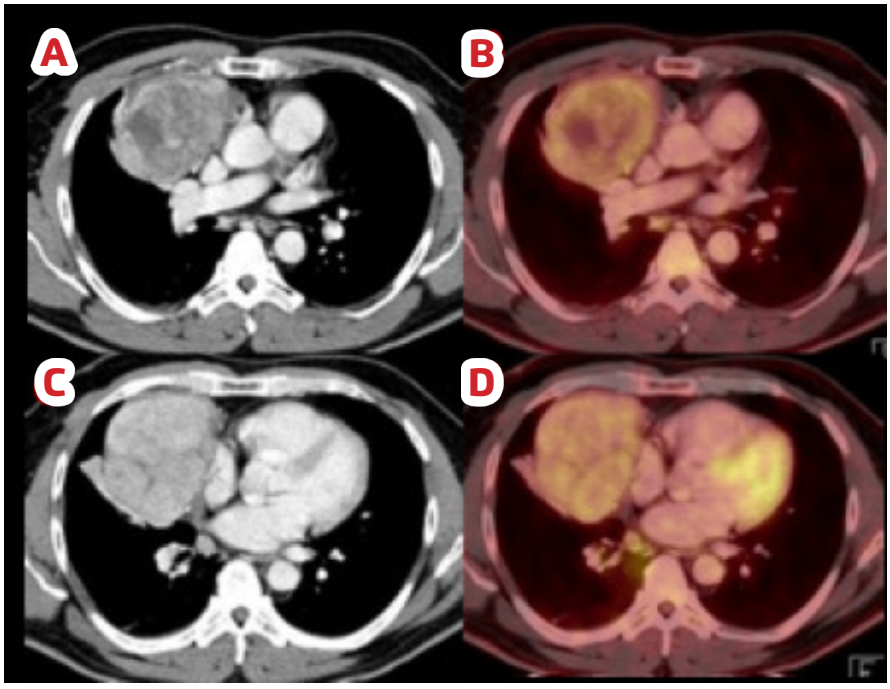

Figure 7.
Axial CT (A & C) and PET-CT (B & D) chest. Prevascular (anterior) mass with heterogenous enhancement and cystic areas within the mass. Slight uptake of FDG, with a SUV max of 4.2. Biopsy through mediastinoscopy revealed a Non-Hodgkin Lymphoma.
References: Radiology Department, Facultad de Medicina UDD-CAS, Clinica Alemana de Santiago - Santiago/CL

Conclusion

It is important for radiologists to be aware of the many appearances of thymic pathology, and how to accurately approach those that need to be treated. PET-CT is an important contributor to a proper diagnosis.

References

1. *Bogot NR, Quint LE. Imaging of thymic disorders. Cancer Imaging. 2005; 5:139-149.*
2. *Sharma P, Singhal A, Kumar A, Bal C, Malhotra A, Kumar R. Evaluation of thymic tumors with 18F-FDG PET-CT: a pictorial review. Acta Radiol. 2013; 54:14-21.*
3. *Liu Y. Characterization of thymic lesions with F-18 FDG PET-CT: an emphasis on epithelial tumors. Nucl Med Commun. 2011; 32:554-562.*
4. *Cheson BD. Role of functional imaging in the management of lymphoma. J Clin Oncol. 2011; 29:1844-1854.*
5. *Schöder H, Noy A, Gönen M, Weng L, Green D, Erdi YE, Larson SM, Yeung HW. Intensity of 18Fluorodeoxyglucose uptake in positron emission tomography distinguishes between indolent and aggressive non – Hodgkin's lymphoma. J. Clin Oncol 2005; 23:4643-4651.*

Abstract 13.

The prostate anatomy, a useful tool for clinical practice: assessed through augmented reality

María Fernanda Tapia,
Daniel Hasson,
Andrés Labra Weitzler.

Clinica Alemana de Santiago, RM/CL

Presentado en European Congress of Radiology, 28 febrero – 4 marzo 2018 Viena, Austria.
Presentación oral

Learning objectives

- To reduce the imprecision of the location of prostatic lesions.
- Describe the prostate anatomy in magnetic resonance through augmented reality.

Background

Prostate cancer is a substantial public health problem worldwide. It is the most common neoplasm among men and third-ranked cause of cancer death in Europe, with almost 400.000 cases and over 92.000 deaths. According to the data of Chile, there is an approximate mortality rate for prostate cancer of 17.2 per 100,000 inhabitants per year, being the second most common cause of death due to neoplasia in our country [1].

The introduction and widespread use of the Prostate specific Antigen testing (PSA) strongly modified the epidemiology of prostate cancer. Although it turned effective in reducing prostate specific mortality, the relevant over diagnosis and the side effects of treatment, it became necessary to use other diagnostic methods such as magnetic resonance imaging [1].

The timely management of this pathology, allows improving the quality of life of the patient, reducing mortality and

reducing costs associated with treatment. In the radiologist's practice it is very important to describe the lesions, their location and the appropriate terminology, in order to have a greater consensus with the clinician and provide a more precise treatment with the best possible results [1].

The prostate is divided into 4 histological zones, the central zone, the transition zone, the peripheral zone and the anterior fibromuscular stroma.

- The peripheral zone comprises 70% of the gland and extends from the base to the apex of the prostate.
- The central zone is located at the base of the prostate, between the peripheral zone and the transition zone, includes 25% of the gland and surrounds the ejaculatory ducts.
- The transition zone forms 5% of the gland and is represented by 2 lobes that surround the proximal prostatic urethra.
- The anterior fibromuscular stroma corresponds to the anterior external surface of the prostate.

In the posterolateral aspect of the prostate, the neurovascular bundle is observed, which represents an important topic, as it is a path of neoplastic dissemination [2].

Findings and procedure details

- **Augmented reality**

Is a live view of a physical, real-world environment related to elements generated by computer. It allows users to experience their surroundings at the same time they are viewing virtual information. Virtual reality unlike the augmented reality replaces the real world with a simulated one.

Augmented reality supplements the real world with virtual objects that appears to coexist in the same space as the real world.

With the help of advanced AR technology, the information about the surrounding real world becomes interactive and digitally manipulable [3].

- **Education and augmented reality**

Students can use augmented reality to construct new understanding based upon their interactions with virtual objects, which bring underlying data to life [3].

Conclusion

- The division of the prostate gland and associated structures in sectors, standardizes the reports and facilitates the precise location of magnetic resonance guided biopsies, improving the therapy, the pathological correlation and the result of the surgery [2].
- Augmented reality provides opportunities for more authentic learning, giving students a more personalized and explorative learning experience.
- AR is in the early stages of application within healthcare education but it has enormous potential for promoting learning experience, achieving core competencies, such as decision making and effective teamwork in healthcare [3].
- This technological tool can be used for interactive learning techniques on simulation of procedures, among others [4].

Personal information

References

1. *F.H. Schröder, J. Hugosson, MJ. Roobol, et al. Screening and prostate cancer mortality: results of the European Randomised Study of Screening for Prostate Cancer (ERSPC) at 13 years of follow-up. Lancet .2014; 384:2027–2035.*
2. *K. Hammerich, G. Ayala, T. Wheeler. Anatomy of the prostate gland and surgical pathology of prostate cancer. Part of Contemporary Issues in Cancer Imaging. Cambridge University press, Dec. 2008.*
3. *D. Douglas, C. Wilke, J.D. Gibson, et al. Augmented Reality: Advances in Diagnostic Imaging. Multimodal Technologies and Interact. 2017;1:29.*
4. *E. Siegel, V. Gupta. Augmented Reality Technology Poised to be a Game-Changer in Radiology. RSNA news. July 1, 2017.*
5. *L. Soler, S. Nicolau, J Schmid, C. Koehl, et al. Virtual Reality and Augmented Reality in Digestive Surgery. ISMAR. 2004. 64; 278-279- 10.1109.*

Abstract 14.

ITMIG classification of mediastinal anatomy: exposure through augmented reality

María Fernanda Tapia[1],
Daniel Hasson[2],
Julia Alegría[1].

[1] Santiago/CL, 2Santiago de Chile/CL

Presentado en European Congress of Radiology, 28 Febrero – 4 Marzo, 2018 Viena, Austria.
ECR 2018 / C-1392

Learning objectives

- To make known the ITMIG classification in the radiological community.
- To reduce the inaccuracy of the location of pathologies in the mediastinum.
- To show through CT images and interactive illustrations with augmented reality, the new classification of mediastinal anatomy.

Background

The division of the mediastinum into compartments is useful for an adequate identification, characterization and management of mediastinal pathologies. The most widely used classification is based on the division of the mediastinum through lateral x-ray anatomy, however, the evaluation and management of mediastinal pathology is based mainly on computed tomography (CT) and magnetic resonance imaging. The ITMIG (International Thymic Malignancy Interest Group) classification system seeks to provide a system for cross-sectional images based on anatomical structures, comprising 3 compartments of the mediastinum [1].

1.1 Prevascular compartments: The boundaries are defined by

- Superiorly: Thoracic inlet.
- Inferiorly: diaphragm.
- Anteriorly: the posterior border of de sternum.
- Laterally: parietal mediastinal pleura
- Posteriorly: the anterior aspect of the pericardium as it wraps around the heart.

The mayor contents of this compartment include the thymus, fat, lymph nodes and the brachiocephalic vein.

The most common abnormalities found in the prevascular compartment include:

- Thymic lesions: cyst, hiperplasia, and malignancy such as thymoma, thymic carcinoma and neuroendocrine neoplasm.
- Germ cell neoplasm.
- Lymphoma.
- Metastatic lymphadenopathy.
- Intrathoracic goiter [1].

1.2 Visceral Compartments: the boundaries are defined by

- Superiorly: Thoracic inlet.
- Inferiorly: diaphragm.
- Anteriorly: the posterior boundaries of the prevascular compartment.
- Laterally: parietal mediastinal pleura.
- Posteriorly: Vertical line 1 cm posterior to the anterior margin of the spine.

The mayor contents of this compartments include

- Vascular structures: The heart, superior vena cava, ascending thoracic aorta, aortic arch, intrapericardial pulmonary arteries and thoracic duct
- Nonvascular structures: traquea, carina, esophagus and lymph nodes.

The most common abnormalities found in the visceral compartment include

- Lymphadenopathy: lymphoma and metastatic disease.
- Duplication cysts.
- Traqueal lesions.
- Esophageal neoplasm.
- Vascular lesions arising from the heart, pericardium and great vessels [1].

1.3 Paravertebral Compartments: the boundaries are defined by

- Superiorly: Thoracic inlet.
- Inferiorly: diaphragm.
- Anteriorly: the posterior boundaries of the visceral compartment.
- Laterally: parietal mediastinal pleura.
- Posteriorlaterally: a vertical line along the posterior margins of the chest wall at the lateral aspect of the transverse processes.

The mayor contents of this compartments include

- Thoracic spine.
- Paravertebral soft tissues.

The most common abnormalities found in the visceral compartment include:

- Neurogenic neoplasm: that arise from the dorsal root ganglia.
- Infectious: discitis and osteomyelitis.
- Traumatic origin: hematoma.
- Miscellaneous lesions: extramedullary hematopoiesis [1].

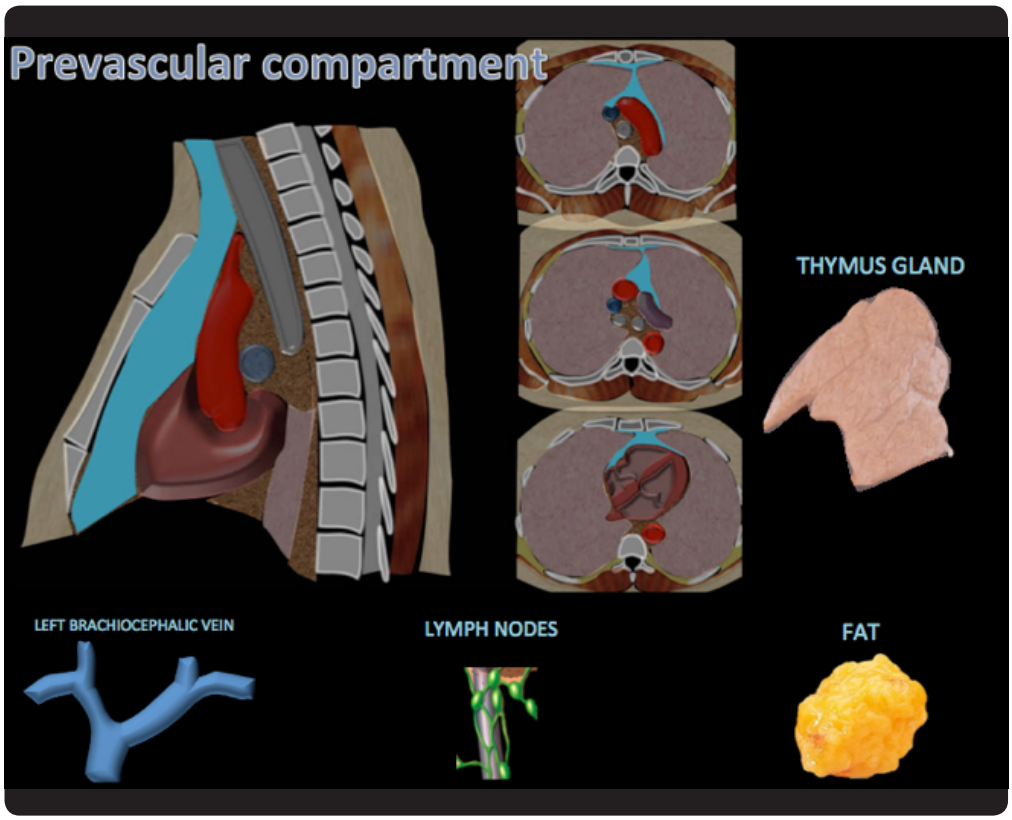

Figure 1.
Prevascular compartment ilustration. The mayor contents of this compartment include the thymus, fat, lymph nodes and the brachiocephalic vein. References: - Santiago/CL

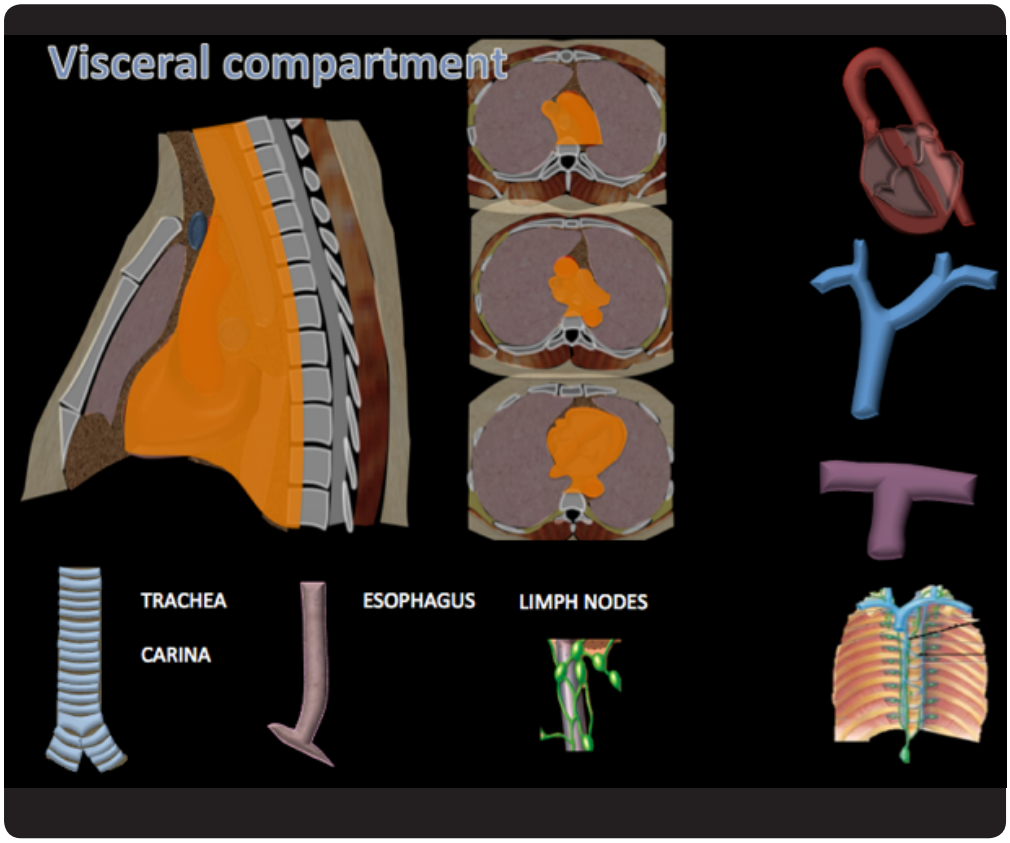

Figure 2.
Visceral compartment ilustration. The mayor contents of this compartments include • Vascular structures: The heart, superior vena cava, ascending thoracic aorta, aortic arch, intrapericardial pulmonary arteries and thoracic duct • Nonvascular structures: traquea, carina, esophagus and lymph nodes. References: - Santiago/CL

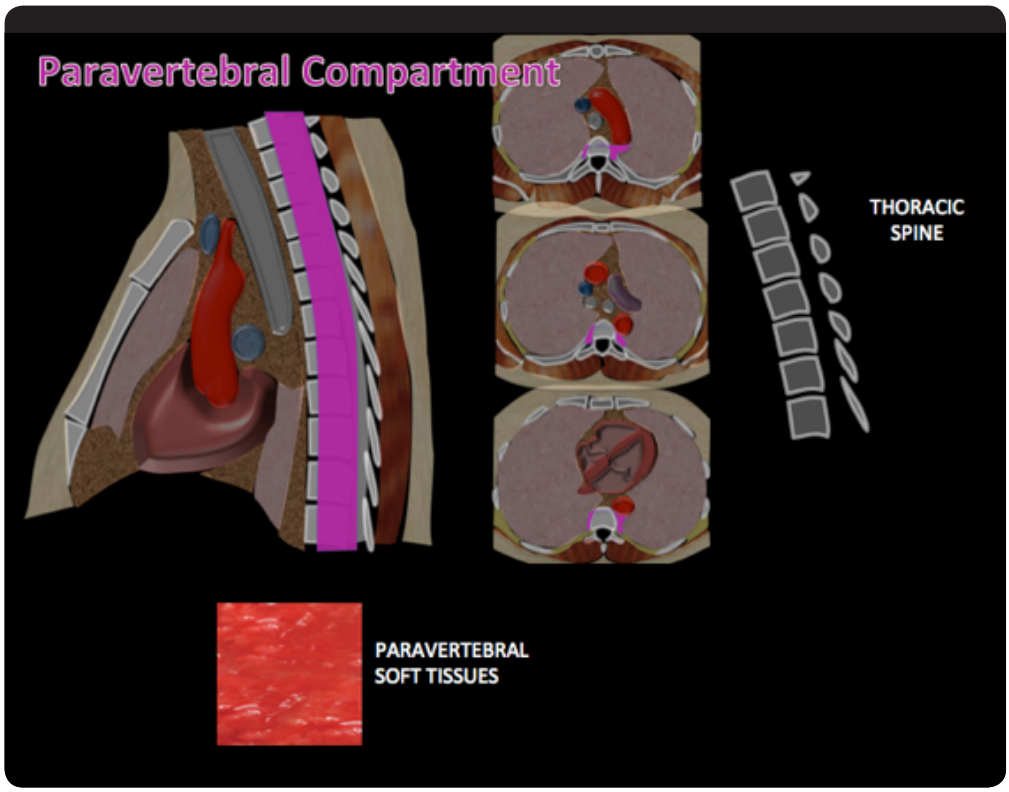

Figure 3.
Paravertebral compartment ilustration. The mayor contents of this compartments include thoracic spine and paravertebral soft tissues. References: - Santiago/CL

Findings and procedure details

Augmented reality

Is a live view of a physical, real-world environment related to elements generated by computer. It allows users to experience their surroundings at the same time they are viewing virtual information. Virtual reality unlike the augmented reality replaces the real world with a simulated one.

Augmented reality supplements the real world with virtual objects, which appear to coexist in the same space as the real world.

With the help of advanced augmented reality technology, the information about the surrounding real world becomes interactive and digitally manipulable [2-3].

Education and augmented reality

Student can use augmented reality to construct new understanding based upon their interactions with virtual objects, which bring underlying data to life[2-3].

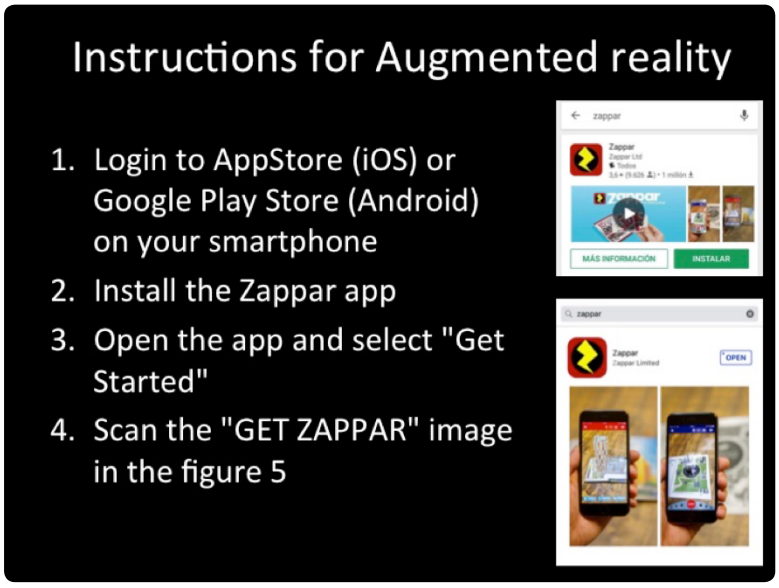

Figure 4.
Augmented reality instructions. 1. Login to AppStore (iOS) or Google Play Store (Android) on your smartphone 2. Install the Zappar app 3. Open the app and select "Get Started" 4. Scan the "GET ZAPPAR" image in the Figure 5. References: - Santiago/CL

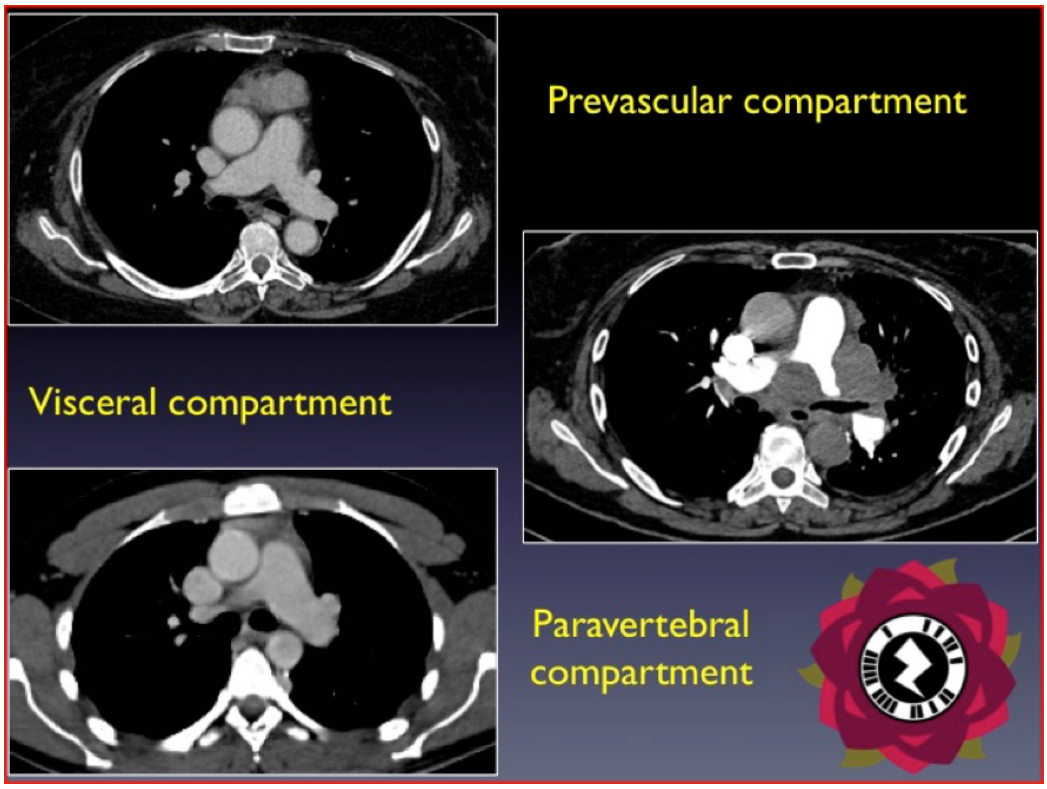

Figure 5.
Tracking image for augment reality. In the prevascular compartment an homogenous mass corresponding to a thymoma is observed. In the visceral compartment a multiple masses corresponding to a Mediastinal adenopathy for lymphoproliferative disease is observed. In the paravertebral compartment a mass adjacent to the vertebral bodies corresponding to a neurogenic tumor is observed. References: - Santiago/CL

Conclusion

- The mediastinum contains vascular, non-vascular structures and organs. It is located in the center of the thoracic cavity. The ITMIG classification system separates the mediastinum into 3 compartments: the pre-vascular, the visceral and the paravertebral. Images are presented that exemplify their limits, modification of spaces in relation to mediastinal masses and the tools of the ITMIG system are presented for the identification of the origin compartment in lesions in which this is doubtful.
- Augmented reality provides opportunities for more authentic learning, giving students a more personalized and explorative learning experience.
- Augmented reality is in the early stages of application within healthcare education but it has enormous potential for promoting an authentic learning experience, achieving core competencies, such as decision making and effective teamwork in healthcare.
- This technological tool can be used for interactive learning techniques on simulation procedures, among others.

References

1. *B. Carter, M. Benveniste, R. Madan, M. Godoy, et al. ITMIG Classification of Mediastinal Compartments and Multidisciplinary Approach to Mediastinal Masses.RadioGraphics201737:2,413-436.*
2. *D. Douglas, C. Wilke, J.D. Gibson, et al. Augmented Reality: Advances in Diagnostic Imaging. Multimodal Technologies and Interact. 2017; 1: 29.*
3. *E. Siegel, V. Gupta. Augmented Reality Technology Poised to be a Game-Changer in Radiology. RSNA news. July 1, 2017.*

Abstract 15.

Role of ultrasound in management of indeterminate thyroid nodules (Bethesda III and IV)

Eleonora Horvath, Camila de la Barra, Guillermo Aguilera, Claudio Silva, Jeannie Slater, Velimir Skoknic, Sergio Majlis, M. Garcia, Paulina González.

Santiago/CL

Presentado en European Congress of Radiology, 28 febrero – 4 marzo 2018 Viena, Austria.
PREMIADO COMO MEJOR TRABAJO EN CABEZA Y CUELLO.

Abstract

Purpose: To evaluate the role of US in predicting benignity or malignancy of lesions decisions (follow-up, re-puncture or surgery).

Methods and materials: IRB approved retrospective descriptive study. Thyroid fine needle aspirations (FNA) with clot technique, performed between 2010-2015 were reviewed. Nodules classified as Bethesda III (Atypia of Undetermined Significance = AUS; Follicular lesion of undetermined significance = FLUS) and IV (Follicular Neoplasm = FN and Suspicion of Follicular Neoplasia = SFN) were selected. Only patients who underwent thyroidectomy were included for thig analysis. Nodules were considered low risk on US when presenting as TIRADS score 2, 3, 4A and intermediate-high risk with TIRADS 4, 48, 5, US risk was compared with the presence of malignancy in the surgical specimen.

Results: In total 3.738 FNAs were performed in the period studied; 269 (7,2%) were Bethesda III and 46 (1.2%) Bethesda IV. Ninety patients (65 FLUS, 11 AUS and 14 FN/SFN) underwent surgery. In TIRADS 4, 4B and 5 nodules malignancy was 12,2% (6/49) in FLUS, 100% (10/10) in AUS and 50% (6/12) in FN/SFN. Meanwhile, in TIRADS 2, 3 and 4A nodules, no malignancy was identified (0/19).

Conclusion: The high presence of AUS malignancy is highlighted. No malignancy was detected for Bethesda III-IV nodules presenting with low risk US TIRADS patterns. This information could assist the clinician on making therapeutic decisions.

Abstract 16.

Breast Fibromatosis Imaging Patterns Mimicking Breast Carcinoma -» Emphasis on Young Women

Eleonora Horvath, Mónica Rochels, Claudio Silva, Miguel Angel Pinochet, Cecilia Galleguillos, Flavia Pizzolon, Valentina Villalón, Marcela Uchida, Eduardo Soto.

Santiago/CL

Presentado en European Congress of Radiology, 28 febrero – 4 marzo 2018 Viena, Austria.
P-3163-ECR Scientific Paper

Abstract

Purpose: To describe the clinical, radiological and pathological features observed in our series of 12 cases of primary Breast Fibromatosis (BF), a rare, benign stromal tumor.

Methods and materials: IRB approved retrospective descriptive study, Clinical presentation, imaging and histopathological findings for each case of BF diagnosed by US-guided biopsies in a period of 8 years were analyzed.

Results: Twelve cases were identified with ages ranging from 17|to 66 years old. Distinct patterns were evident according to clinical conditions and age of presentation:

- Recent breast implants: 4 women with implants (prior surgery 1 to 5 years 290) presented las hypoechoic vascularized, aggressively growing masses.
- Older than 25 years: 5 patients (P5-56 years). BF presented as a suspicious solid, unilateral breast mass, two cases mimicked malignancy (B-RADS 5) in all imaging modalities.
- Younger than 25 years: 3 patients (17-21 years). BF presented as rapidly growing multifocal, bilateral, palpable masses with nipple retraction.

All US had highly suspicious irregular, poorly marginated, hypoechoic, vascularized lesions ranging from 2-5 cm. MRI showed a multifocal- bilateral non-mass enhancement after injection of gadolinium.

After surgery and a follow-up period ranging from 1 to 65 months all patients are disease-free. Histologically, these three patterns are identical, characterized by an infiltrating, loose spindle cell proliferation, with fibroblastic cells and variable amounts of extracellular collagen and scant lymph: infiltrates.

Conclusion: Breast fibromatosis, though pathologically alike, in very young women has a clinical and radiological presentation different to what is known and classically reported in the literature.

Abstract 17.

Ultrasonographic Diagnosis of Salivary Gland Atrophy after Radio-iodine Treatment for Papillary Thyroid Cancer

Eleonora Horvath, Velimir Skoknic, Claudio Silva, Hernán Tala, Nicolás Sánchez, Carolina Whittle, Juan Pablo Niedmann, Sergio Majlis, C. Schweinitz

Santiago/CL

Presentado en European Congress of Radiology, 28 febrero – 4 marzo 2018 Viena, Austria.
P-4328-ECR Scientific Paper

Abstract

Purpose: To describe ultrasonographic (US) findings of mayor salivary glands (MSG) atrophy in patients who received radio-iodine (RAI) treatment for papillary thyroid cancer (PTC). Determine MSG damage prevalence and associated risk factors.

Methods and materials: IRB approved, prospective non-concurrent cohort study. Patients that had CPT surgery with subsequent RAI between 2005-2015, were included. All had a preoperative US and at least one follow-up US 12 months after RAI administration. Patients with prior MSG altered findings were excluded. Uni and multivariate analysis with logistic regression was performed using US gland damage as dependent variable and RAI dose, gender and age as independent variables. Statistical significance was defined as $p<0.05$.

Results: in total 328 patients [average age: 42.47(1QR 34-53), female: 263 (80.2%)] met inclusion criteria, receiving a median dose of 105mCi (IQR 100-150). Follow-up period: 12-107months. In 103 patients (31.4%) US detected salivary gland atrophy (size reduction, wavy contours, hypoechogenicity and heterogenous structure) in at least one MSG. Univariate analysis indicated that total RAI dose received was significantly associated with atrophy ($p<0.01$). No actin injury was present in patients treated with a total dose lower than 100mCi. Multivariate logistic regression revealed total radiation dose OR of 2.35 (1C95% 1.80 to 3.06) and women OR of 2.17 (IC 95% 1.017 to 4.42) for MSG atrophy.

Conclusion: Actinic sialoadenitis is common, affecting approximately one-third of patients. Cumulative dose is the main factor related to this damage. For the first time, US was used to prospectively and systematically evaluate the MSG of patients with RAI treatment.

Abstract 18.

Background parenchymal enhancement at breast magnetic resonance imaging - Association with tumor response to neoadjuvant chemotherapy

Eleonora Horvath, Eliette Castillo, Claudio Silva, Carla Darrás, María Elisa Droguett, Cecilia Galleguillos.

Santiago/CL

Presentado en European Congress of Radiology, 28 febrero – 4 marzo 2018, Viena, Austria.
P-4317-ECR Scientific Paper

Abstract

Purpose: Analyze neoadjuvant chemotherapy (NAC) effect on breast MR (BPE). Determine association between BPE changes and tumor response.

Methods and materials: IRB-approved, analytic retrospective study. All and had pre-treatment and follow-up 3T MARI studies between December BPE was analyzed on subtraction images and axial and sagittal MIP. Tumors were classified according to histology as invasive ductal carcinoma and grouped by immunohistochemical (IHC) subtype: Luminal A, Lumina Triple negative (TN). Imaging response was evaluated using RECIST 1.1

Results: 40 patients were included, mean age of 47 + 9.9 years, 67,5 % were premenopausal.

Histopathological analysis revealed 37 cases of IDC, two ILC and one IDC+ILC. IHC assessment showed 12 TN,10 Luminal A, 10 Luminal B and 8 (HL). There was a global reduction of BPE after NAC in women (Pv= 0.01). TN and HL had higher initial BPE, and postmenopausal women (Pv= 0.001). TN and HL had higher initial BPE, and postmenopausal patients had an OR of 6.4 for having a mild BPE prior to NAC. 32,5% of patients had complete imaging response. Ap A/B 1HC subtype were associated with higher OR for partial tumor response (OR 1.8,2 y 5.7, respectively), although only IHC subtype reached statistical significance.

Conclusion: Decrease in BPE signal after NAC may be used as a predictive factor of tumor response.

Abstract 19.

Can a hyperechogenic breast lesion be malignant?

Eleonora Horvath, Eliette Castillo, Flavia Pizzolon, Claudio Silva, Marcela Gallegos, Miguel Angel Pinochet, Cecilia Galleguillos, Marcela Uchida, Paulina Gonzalez.

Santiago/CL

Presentado en European Congress of Radiology, 28 febrero – 4 marzo 2018, Viena, Austria.
P-4336-ECR Scientific Paper

Abstract

Purpose: Hyperechogenic breast lesions have been described as pa 0d benign and are rarely biopsied. The aim of this work was to evaluate the frequency of malignant hyperechogenic breast lesions, describe their imaging findings and histopathological characteristics.

Methods and materials: IRB approved, retrospective, descriptive case series. Biopsied hyperechogenic lesions were selected from a database of 3.394 consecutive US-guided breast Core biopsies (1,020 malignant, 299 high-risk and 2,075 benign lesions) performed between 2006 and 2016. Any lesion that presented greater echogenicity than subcutaneous cellular tissue of more than 90% of its volume, was considered hyperechogenic. Demographical data, US and histopathological characteristics were recorded.

Results: In total 27 (1,08%) lesions biopsied were hyperechogenic: 21 (57%) of them had benign results.

Sixteen patients (mean age: 52 years; range: 26-80) had hyperechogenic cancer, representing 1,5% (16/1,020) of all malignancies: 1 CDIS and 15 invasive carcinomas (81% ductal and 19% lobular histology). Mean size = 2 cm, range: 7- 30 mm. All of them exhibited a small central hypoechoic foci and were partially or completely surrounded by fatty tissue. Shape, margins, orientation and vascular architecture were highly suggestive of malignancy on US, mammogram and MARI (features BI-RADS 4 and 5). In histopathological exam these cancer$ were surrounded by adipose tissue (not by fibroglandular tissue); also, they presented a hypocellular collagenous center and were hypercellular on ¡ts periphery, intermixing with fatty tissue, fibrous tracts and collagen.

Conclusion: Hyperechogenic cancers are very rare (less than 2% of breast cancers), but it is important to recognize them to avoid misdiagnosis.

Abstract 20.

Kikuchi-Fujimoto disease: report of 5 cases mimicking malignancy in axillary lymph nodes

Eleonora Horvath, Sebastián Villarreal, Claudio Silva, Cecilia Galleguillos, Miguel Angel Pinochet, Valentina Villalón, Marcela Uchida, Heriberto Wenzel, Eduardo Soto.

Santiago/CL

Presentado en European Congress of Radiology, 28 febrero – 4 marzo 2018, Viena, Austria.
P-4311-ECA Scientific Paper

Abstract

Purpose: To describe the clinical, radiological and immunohistochemical features manifested as presence of axillary adenopathies.

Methods and materials: IRB approved retrospective review of axillary adenopathies biopsied with histopathological results of KFD between 2012 - 2017. Demographic, clinical, radiological and histopathological data and immunohistochemical findings were recorded.

Results: In a 5 year-period, five patients (all women, median age 33, ranging from 22 -70) were biopsied for suspicious axillary adenopathies (3 Core and 2 excisional biopsy) with histopathological diagnosis of KFD. All presented palpable axillary masses, two had low-grade fever, and one had nocturnal sweating. Ultrasonography showed moderately enlarged (up to 3 cm), hypoechogenic, vascularized, conglomerated adenopathies (B-RADS 4), unilateral, with no signs of periadenitis, one patient had a CT exam and another PET-CT for suspicious of lymphoma. None of the patients had images suggestive of breast cancer on mammography or US. They also had no known autoimmune manifestations (e.g. lupus erythematous or rheumatoid arthritis), as described in KFD. Histopathology demonstrated histiocytic necrotizing lymphadenitis in all cases (positive staining for CDS and CD20, negative Dí and BCL-2). Medical treatment was offered (NSAID) in three cases and surgical removal on the remaining. Amp more than six months of follow-up and US follow-up showed regression of inflammatory phenomena. No recurrence was observed in this series.

Conclusion: KFD is a self-limiting disease that is increasingly diagnosed dn histology in axillary lymphadenopathies. Awareness of this condition is necessary to avoid unnecessary studies and procedures.

Abstract 21.

Prospective evaluation of extent of disease in prostate cancer biochemical relapse by [68Ga]PSMA-HBED-CC PET/CT

Guillermo Chong, Daniela Barahona, Andrea Balcells, Daniel Hasson, Giancarlo Schiappacasse, Andrés Labra Weitzler.

Santiago/CL

Presentado en European Congress of Radiology, 28 febrero – 4 marzo 2018, Viena, Austria.

Abstract

Purpose: Accurately determining the extent of disease on biochemical relapse of prostate cancer (PCa) can have important therapeutic implications. The lesion detection rate of [68Ga]PSMA-HBED-CC-PET/CT and its relation to prostate-specific antigen (PSA) level and Gleason score is evaluated.

Methods and Materials: All patients subjected to [68Ga] PSMA-HBED-CC-PET/CT with PCa biochemical relapse, from November 2014 to December 2016 were included. Laboratory exams performed prior to PSMA-PET-CT were retrieved from electronic medical records, and histopathology results were extracted from surgical specimens. All high-uptake regions were identified by two experienced readers. Regional involvement was defined as urethrovesical anastomosis lesions or pelvic lymphadenopathies.

Results: 102 patients were recruited. Mean age was 70.3 years (SD: 9.2), and median PSA Score was 2.52 ng/ml (IQR: 7.1), with a minimum value of 0.04 ng/ml, and 35% of PSA values under 1 ng/ml. PSMA-PET/CT was positive for 70% of patients. Among PSMA-PET/CT positive cases, 55% had regional involvement and 2.5% had suprapelvic lymphadenopathies without regional involvement. PSMA-PET/CT was positive in 43% of studies with PSA levels of <1 ng/ml. The lowest PSA level related to a positive finding was 0.11 ng/ml. 16% of lymphadenopathies detected were under 0.5 cm, and 69% were under 1 cm. 28% of studies showed bone metastases. A high Gleason score (9-10) was non-significatively associated with a higher number of pelvic metastases.

Conclusion: [68Ga]PSMA-HBED-CC-PET/CT can identify secondary lesions in PCa biochemical relapse even in patients with very low PSA levels and can accurately identify small intra- and extra-pelvic lymphadenopathies, which can substantially influence treatment planning.

Abstract 22.

Atypical ultrasonographic patterns of papillary thyroid carcinoma: how to recognize them?

Eleonora Horvath, Guillermo Aguilera, Claudio Silva, María Elisa Droguett, Velimir Skoknic, Hernán Tala, Sergio Majlis, Jeannie Slater, Carolina Whittle.

Santiago/CL

Presentado en European Congress of Radiology, 28 febrero – 4 marzo, 2018 Viena, Austria.

Abstract

Purpose: To analyze the atypical papillary thyroid carcinoma (PTC) US patterns, comparing them with typical cases and to describe their main characteristics.

Methods and materials: Retrospective review of thyroidectomies between 2013 and 2016 with PTC. Classical PTCs (Group A) were separated from those that showed atypical patterns (Group B). These were compared according to age, gender, size, histological subtype and association with Hashimoto's thyroiditis (HT). Shapiro-Wilk, chi-2, Students t tests or Mann-Whitney- Wilcoxon tests were used.

Results: A total of 453 PTC met inclusion criteria. In 51 cases (11.2%) [19 men (38%), median age 41 years (14-68)] an atypical pattern was observed. Median size: 14 mm (5-50 mm), 32 (63%)> 10 mm. 27% were associated with HT. A significant difference was found between Groups A and B in terms of gender ($p < 0.025$), size ($p < 0.001$) and histological subgroup ($p < 0.01$), finding more men, larger lesions and more follicular variant of PTC with atypical pattern. The dominant characteristics observed in Group B were: solid-cystic mixed structure, similar to colloid nodule but without hyperechoic foci 23 (45%), isoechogenicity 19 (37%) and presence of capsule 20 (40%), findings that were shared in the majority of the cases, with or without association to calcifications. In addition, pooled microcalcifications without associated nodule were detected in 6 cases (12%).

Conclusion: One in every 10 PTCs has an atypical ultrasound appearance. It is important to recognize the characteristics described as concerning for malignancy in order to recommend FNAs in a timely manner, since 63% are macrocarcinomas.

Abstract 23.

Contribution of pre operative breast MRI study in pure DCIS

Eleonora Horvath, Carla Darrás Ismael, Claudio Silva, Eliette Castillo, Miguel Angel Pinochet, Cecilia Galleguillos, María Elisa Droguett, Valentina Villalon, Flavia Pizzolon.

Santiago/CL

Presentado en European Congress of Radiology, 28 febrero – 4 marzo 2018 Viena, Austria.

Abstract

Purpose: To evaluate the usefulness of preoperative MAI study in patients with pure ductal carcinoma in situ (DCIS).

Methods and materials: IRB approved, retrospective, descriptive observational study, of a series of cases. Patients with breast cancer operated between January 2015 and March 2017 were reviewed and pure DCISs with mammography (Mx), ultrasound (US), and preoperative MRI available in PACS were selected. Bland-Altman test was used to describe the size concordance considering the histopathology of the surgical specimen as the reference standard. The MAI contribution was classified into 4 groups.
Group 1: MARI provided the same information as conventional studies.
Group 2: improved the description of tumor size without changing surgical approach.
Group 3: generated unnecessary procedures.
Group 4: correctly changed the surgical management.

Results: Of 467 cancers operated, 77 (16.5%) were DCIS, 41 (53.2%) pure and 36 with microinvasion (46.8%). Thirty-three patients met inclusion criteria. Average age 52.78 + 12.55 years. The detectability of the lesions was 90.9%, 30.3% and 74.2% for the Mx, US and MARI respectively. Concordance index of tumor size: MRI=73.3%, US=70% and Mx=58.1%. MRI contribution in preoperative staging: Group 1=18 cases (58%), Group 2= 3 cases (9.7%), Group 3=0 and Group 4=2 cases (6,5%).

Conclusion: Undoubtedly Mx is the main method of detection of pure DCIS. However, MAI proved to be the best technique to evaluate tumor size, allowing better pre-operative staging than conventional studies in 15% of cases, even to correctly change surgical management in 6%.

Abstract 24.

Concordance and inter-reader agreement for PIRADS v2.0 in bi-parametric versus multi-parametric prostate MRI approaches

Andrés Labra, Giancarlo Schiappacasse, Daniela Barahona, Claudio Silva

Presentado en European Congress of Radiology, 28 febrero – 4 marzo, 2018, Viena, Austria.

Abstract

Purpose: Biparametric prostate MRI is a desirable approach for screening purposes. A comparison of the concordance of biparametric prostate MRI compared to standard 3T multiparametric MRI is studied.

Methods and materials: 150 cases were retrospectively selected among multiparametric prostate MRI (mpPMRI), with a stratified randomized scheme based on PIRADS v2.0 categories distribution during 2015-2016. Anonymized cases were presented to three independent readers with 5-8 years of experience in prostate MRI. For bi-parametric evaluations, the same cases were used by extracting T2w y DWI series from the original mpPMRI, and presented in a random case sequence to the same readers after 6 weeks. Reader and inter-technique agreement was analyzed using weighted Kappa. 95%CI were estimated when feasible.

Results: Weighted kappa for the three readers was 0.69. The highest agreement was achieved among the most experienced readers, reaching 0.72. Agreement among the least experienced reader and the most experienced ones ranged from 0.680 and 0.675. Agreement for the reading of bi-parametric versus multi-parametric MRI was 0.79, corresponding to a high concordance.

Conclusion: Bi-parametric approach has a high concordance with multiparametric prostate MRI, with a high reader agreement among trained abdominal radiologists, with a fraction of scanner time. This method could aid in detecting lesions with a high confidence, and providing better selection for those that may require a further complete multiparametric MRI (e.g. prior to fusion biopsy of a suspicious lesion).

Abstract 25.

Abdominal pain: when the abdomen does not speak, the chest screams

Daniel Schneider [1], Fabián Villacrés [1], Julia Alegría [2], Claudio Silva [2].

[1] Resident. Department of Radiology, Clínica Alemana Santiago - Universidad del Desarrollo.
[2] Radiologist. Department of Radiology, Clínica Alemana Santiago - Universidad del Desarrollo.

Presentado en 2018 ARRS Annual Meeting, 22-27 abril, Washington DC, Estados Unidos.

Background Information/Purpose

Visceral pain is mediated by nociceptors in the cardiovascular, respiratory, gastrointestinal and genitourinary systems; usually described as deep, oppressive or colicky pain and is commonly referred to cutaneous sites, since the somatic and visceral structures have dual innervation, with common afferent fibers converging on the dorsal horn of the spinal cord. This pain results from the mechanical or chemical activation of the nociceptors, either by tumor compression, visceral distention or obstruction. The irritation of the diaphragmatic pleura is probably one of the main causes of abdominal symptoms in patients with thoracic pathology, it being important to keep in mind that some of these conditions may be visible in the lower thorax segment in an abdominal tomographic study.

Educational Goals/Teaching Points

To provide a pictorial review of some critical incidental chest findings on computed tomography requested for abdominal pain.

To describe the pathophysiology of abdominal pain of thoracic etiology.

To review the tomographic findings of thoracic conditions that can cause abdominal pain, such as of myocardial infarction, ventricular rupture, epipericardial fat necrosis and pulmonary embolism. To discuss the importance of not forgetting to check the inferior segment of the chest in abdominal computed tomography, to look for possible thoracic causes of abdominal pain.

Key Anatomic or Pathophysiologic Issues, Imaging Findings or Imaging Technique

Case 1: 84 yo male. Abdominal pain. Acute pancreatitis suspected.

NECT: Subendocardial fat in the lateral wall of the left ventricle representing healed myocardial infarction.

CECT: Myocardial hypoenhancement in the lateral, septal and anterior wall of the left ventricle and papillary muscle, indicative of myocardial ischemia.

Case 2: 62 yo male. Medical history of diabetes. Abdominal pain and vomiting.
CECT: Enhancement defect in the anteroseptal wall of left ventricle. Filling defect in the left ventricular apex that suggests the presence of a thrombus.

Case 3: 83 yo female. Abdominal pain.
CECT: Hypoenhancement and rupture of the anterior wall of the left ventricle. Hemopericardium is also visible. Pericholecystic fluid, gallbladder wall thickening and a gallstone in the gallbladder.

Case 4: 57 yo female. Abdominal sepsis.
CECT: Filling defect in the left and right lower lobe segmental branches. Consolidation in the lateral segment of the left lower lobe representing lung infarction.

Case 5: 54 yo. Female. Epigastric pain and vomiting.
CECT: The left epicardial fat pad shows inflammatory stranding (yellow arrow) and contains a 30mm ovoid encapsulated fatty lesion.

Conclusion
Abdominal pain may be the only manifestation of a thoracic pathology, which is sometimes life-threatening, and can be identified in the lower segments of the chest on an abdominal computed tomography, so we emphasize the importance of not forgetting to carefully review this area.

Abstract 26.

Three cases of Skene's gland cyst at pediatrics age

Andrea Pichott Fontalba[1], Andrés Retamal Caro[2], Javiera Aguirre Fernández[1], Lizbet Perez-Marrero[1], Isabel Fuentealba Tapia[1]

[1] Clinica Alemana Santiago, Universidad del Desarrollo, Imágenes, Santiago, Chile
[2] Clinica Alemana Valdivia, Imagenología, Valdivia, Chile

Presentado en 40th Post Graduate Course & 54th Annual Meeting of the European Society of Paediatric Radiology (ESPR), 18–22 junio 2018, Berlín, Alemania.

Abstract

Objective: To illustrate the imaging features of Skene´s cysts. Three pediatrics cases are reported at different age.

Case 1: Female newborn with a superficial interlabial yellowish cyst, detected in physical examination with no symptoms.

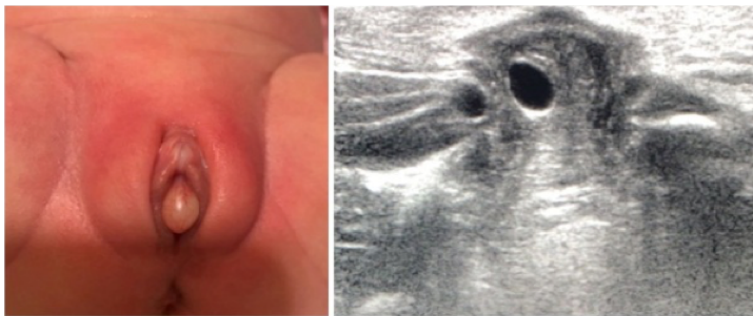

Case 2: Two-year-old girl, left monorrenal. Presentation of a cystic mass adjacent to the vaginal opening.

Case 3: Fifteen-year-old teenage healthy girl, presents two episodes of urinary infection and a cystic lesion which protrudes in the interlabial area.

Discussion: Skene`s gland or paraurethral gland are homologous to the male prostate gland. The cysts of these glands are very rare congenital anomaly in females, which are included in the differential diagnosis of interlabial cysts. Several interlabial masses, including those of embryo- logical origin, ectopic tissue, prolapse, urological anomaly, or neoplasia, can superficially resemble simple cysts. The paraurethral gland cyst is one of the most common neonatal interlabial cysts.

However, cases in older children have also been reported. Perineal ultrasound plays a leading role in the evaluation of pediatric patients, along with MRI in complex cases, which allow characterization of the lesion and its relationship with adjacent structures and an adequate differential diagnosis, which includes prolapse of ectopic ureterocele, cyst of Gartner, hydrometrocolpos associated with an imperforate hymen and botryoid rhabdomyosarcoma.

Abstract 27.

Vascular lymphatic malformations in paediatrics: Radiologic findings

Javiera Aguirre Fernández[1], Andrea Pichott Fontalba[1], Lizbet Perez-Marrero[2], Isabel Fuentealba Tapia[2], Carolina Whittle[3]

[1]Facultad de Medicina Clínica Alemana de la Universidad del Desarrollo, Paediatric Radiology, Santiago, Chile
[2]Clinica Alemana de Santiago, Paediatric Radiology, Santiago, Chile
[3]Clinica Alemana de Santiago, Radiology, Santiago, Chile

Presentado en 40th Post Graduate Course & 54th Annual Meeting of the European Society of Paediatric Radiology (ESPR), 18–22 junio 2018, Berlín, Alemania.

Abstract

The lymphatic vascular malformations (LVM) are consequences of the congenital obstruction of the lymphatic drainage, being the lymphatic vessels sequestered and not communicated with the venous system, its incidence is low, of 1: 12,000 live births, but the majority are manifested in the pediatric age, between 50-65% are detected at birth and 90% diagnosed before 2 years.

Currently they are classified within vascular anomalies as a low-flow vascular malformation and not as a tumor, so the terms lymphangioma or hygroma to name them are obsolete.

Diagnostic images allow classification according to the size of the cysts in microcystic, macrocystic and mixed, which is significant to decide the treatment. They also allow to detect complications, to make differential diagnosis, support percutaneous treatment and follow up. The use of ultrasound with Doppler is an ideal and first-line method, however in the extensive, deep, multicompactorial LVM, which are in relation to vital organs, MRI is the study of choice in children. Computed tomography (CT) also allows the characterization of these anomalies, its use is in the diagnosis, when we study a mass of etiology not specified, however, by ionizing radiation should be avoided its use in the pediatric age.

We present images of US, CT and MRI, including fetal MRI (Figure), representative cases of LVM isolated or associated with syndromes or other anomalies.

Fig N°5. Axial T2, B. Axial T1 Fast Sat, C. Axial T1 Gd. VLM in the left posterior cervical space, a multicystic lesion is observed with liquid - liquid levels and a hypointense focal area in T2 that is hyperintense in T1 that corresponds to blood. In the study with contrast a fine enhancement of its septa is observed.

Abstract 28.

Appendicular lymphoid hyperplasia, differential diagnosis of acute appendicitis: Ultrasound findings

Carolina Whittle, Lizbet Perez-Marrero, Marcela Cortés, Margarita Switt, Javiera Aguirre Fernández.

Clinica Alemana Santiago, Universidad del Desarrollo, Imágenes, Santiago, Chile

Presentado en 40th Post Graduate Course & 54th Annual Meeting of the European Society of Paediatric Radiology (ESPR), 18–22 junio 2018, Berlín, Alemania. Presentación oral.

Abstract

Objectives: To describe ultrasound (US) findings of lymphoid hyperplasia of the appendix (ALH). To report demographic data of patients with ALH operated for acute appendicitis (AA).

Materials and methods: Retrospective, descriptive and observational study. We reviewed biopsies reports of 694 consecutive cases of AA surgeries, who had previous US in our institution. All cases with histopathological ALH diagnosis were selected. Two US experts in consensus described US findings. Age and sex composition of this group were described.

Results: 25 ALH cases (3.8% of all appendectomies), 10 women and 15 men. The average age was 13 years (range 4 - 41 years), 36% under 10 years old and 84% under 20 years old. In all cases ALH was confirmed by biopsy. 22 cases of them without inflammation and 3 cases with associated inflammatory infiltrate of the appendix. The appendix was visualized by US in 22 cases. The average diameter of the appendix was 7 mm. US findings were increase in appendiceal diameter (82%), hypoechogenic pseudonodular submucosal thickening (50%), concentric parietal thickening with endoluminal gas(13%), peri- appendiceal inflammatory changes(18%) and increased wall vascularization(4.5%). In 4 cases appendix was normal in US, 2 associated with intestinal intussusception.

Conclusion: ALH is frequent in children and can predispose to AA. Both pathologies can increase the appendiceal diameter. In the pediatric group, hypoecogenic pseudonodular submucosal thickening in absence of peri-appendiceal inflammatory changes can suggest AHL.

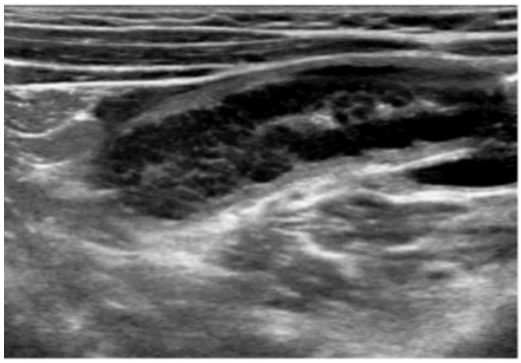

4 years old boy with histopathologic diagnosis of ALH. US shows hypoechogenic pseudonodular submucosal thickening of appendix.

Abstract 29.

Current hepatitis A outbreaks in men who have sex with men - Epidemiological situation in HIV patients in Chile

Claudia Cortés[1,2], Marcelo Wolff[1,2], Luis Miguel Noriega[3], Alejandra Marcotti[3], Carla Palavecino[1], Pía Mateluna[3], Lorena Porte[3], Thomas Weitzel[3]

[1]University of Chile School of Medicine, Medicine, Santiago, Chile,
[2]Fundacion Arriarán, Santiago, Chile,
[3]Clínica Alemana, Facultad de Medicina Clinica Alemana, Universidad del Desarrollo, Santiago, Chile

Presentado en 22nd International AIDS Conference (AIDS 2018), 23-27 julio 2018, Amsterdam, Netherlands.

Background: In 2017, various countries in Europe and the Americas (including Chile) experienced outbreaks of hepatitis A virus (HAV) infections in men who have sex with men (MSM). In Chile, the rate of hepatitis A susceptibility in this population is unknown. Hepatitis A vaccines are available, but not widely used. Our study aimed to analyze the epidemiology of feco-orally transmitted viral hepatitis (A and E) in HIV patients in Santiago, Chile.

Methods: The study used preserved samples from a previous cross-sectional multicenter hepatitis B study in adult HIV patients attending public (Fundación Arriarán, FA) and private health centers (Clínica Alemana, CA) in Santiago. Specimens were tested for antibodies against hepatitis A (Elecsys® anti-HAV total, Roche) and hepatitis E (recomWell HEV IgG, Mikrogen). Demographic, clinical and laboratory data were obtained from medical records.

Results: A total of 394 patients (FA, 348; CA, 46) were included (93% male). Median age was 38 years and 99% acquired HIV sexually (83% MSM, 17% heterosexual). 15% had AIDS and 96% were on ART. In 79%, HIV viral load was undetectable and median CD4 cell count was 499 cells/µL. Of all patients, 77% (CI95%, 72-81%) were HAV seropositive (FA, 79% [74-82%]; CA, 65% [51-77%]). Patients born before 1960, in the 1960s, and the 1970s had high HAV seroprevalences of 97%, 92%, and 87%, respectively. Those born in the 1980s had intermediate (64%) and those born in the 1990s very low rates (18%). Overall seroprevalence of hepatitis E was 10.4% (7.7-13.8%), age-dependently ranging from 18% (born before 1960) to 0% (born in 1990s).

Conclusions: Our study highlights that a large proportion of HIV-patients of younger generations are susceptible to HAV. For risk groups such as MSM, vaccination should therefore be provided to control the current outbreak and prevent further spread. More patients of the private health sector in Chile are HAV susceptible, reflecting the more hygienic living conditions, but also the underuse of vaccination. Surprisingly, we detected hepatitis E antibodies in more than 10% of the study population. The epidemiology and clinical relevance of HEV, which has not been described HIV-patients in Chile, requires further studies.

Abstract 30.

Validation of a model predicting graft survival after liver transplantation: The Donor risk index (DRI) a useful tool in Latin America.

Rodrigo Zapata, Alexandra Ginesta, Monserrat Rius, Fernando Gómez, Edgar Sanhueza, Jorge Contreras, Roberto Humeres, Guillermo Rencoret, Marcelo Vivanco, José Manuel Palacios.

Unidad de Trasplante Hepático. Clínica Alemana de Santiago.
Facultad de Medicina, Universidad del Desarrollo. Santiago, Chile.

Presentado en XXV Congreso Latinoamericano de Hepatología, 20-23 de septiembre de 2018, Punta Cana, República Dominicana.

Background: Orthotopic liver transplantation (OLT) is the only life-saving option for end-stage liver disease patients (pt). The progressive organ shortage and an increase in the waiting list, has led to the use of marginal organs. The development of objective scores to assess the donor (D) is necessary. The Donor Risk Index (DRI) developed in 2006 (Feng et al. Am J Transp), considers seven D characteristics (age; height, graft type, race, cause of death, cold ischaemia time, organ location, donation after cardiac death), and has shown to predict pt/graft failure at 3, 12 and 36 months after OLT in some North American and European centers. Nevertheless, there is still debate on its clinical usefulness and there is scarcity of data in Latin-America.

Aim: To assess and validate DRI as a prognostic model of survival after OLT in Chile with current MELD-based liver allocation rules.

Methods: All adult OLT performed in Clínica Alemana between January/ 2001- May/2017 were included. Biodemographic and clinical data from D and recipients (R) were analyzed from a prospectively built database. The DRI was calculated as described by Feng et al. (Iphone app "Liver DRI"). Statistical analysis through survival curves, and comparisons between groups (t student; p<0,05).

Results: 155 OLT with all complete data, were analyzed. Overall pt survival at 3, 12 and 36 months was: 94%, 91% and 85% respectively.

R data: (Table). D Data: (Table) 68% D were Local and close to OLT center (< 50 km); 17% Regional (51-200 km) and 14% National (>200 km away). Local D had a shorter ischemia time (6,55+0,08 hrs) than Regional or National D (8,09+0,1 and 8,56+0,09 hrs, respectively, p< 0,0001). Mean DRI from Local D (1,28+0,24) was significantly lower than DRI from National D (1,63+0,27; P < 0,0001). A D with a DRI < 1,5 (given to R with a mean MELD score:20,6 points) correlated with a 3, 12 and 36 months survival of 94%, 93% and 88% respectively. A D with a DRI > 1,5 (given to R with a mean MELD score:18,5 points) correlated with a significantly lower pt survival of 90%, 86% and 77% respectively (p=0,02).

	Recipient data	Donor Data	P
Age (y)	51,3 + 11,5 (23% > 60y)	40,9 + 13(29% > 50 y)	P<0,001
Gender	57% men	59% men	NS
Features	• 72%: decompensated cirrhosis • 12%: fulminant hepatitis. • 48%: Child-Pugh C • MELD at OLT: 20+8,5 points • MELD > 22 : 30%	• Height: 167,5 + 8,9 cm • 58%: cerebrovascular accident. • 38%: head trauma. • Mean DRI 1,4 • Ischemia time: 7,24+0,09 hours	

Conclusions: Based on this cohort experience from Chile, a lower DRI score is significantly correlated with a better survival prognosis in pt after OLT. This correlation is also true for higher MELD score R. The use of this score can be very helpful to allocate organs, considering also the D characteristics and especially the regional distances to bring an organ without sacrificing the future allograft function.

Abstract 31.

A quality improvement initiative: the quest for zero Central Line-associated Bloodstream Infections (CLABSI) in hospitalized infants in a Neonatal Intensive Care Unit (NICU) in Chile

Juan Carlos Muñoz MD[1], Beatriz Milet MD[2], Marcela Gómez RN[3], Antonieta Vicentelo RN[4], Marta Contreras RN[5], Marissa Garrido RN[6], Carolina Avila RN[7], Pablo Gaete MD[8], Marcial Osorio MD[9]

[1-9]Clínica Alemana, Santiago, Región Metropolitana, Chile
mmilet@alemana.cl

Presentado en Annual Quality Congress Vermont Neonatal Network, 20 al 24 de septiembre de 2018, Chicago, Estados Unidos.

Setting

This quality improvement project was performed at a level IV non-profit hospital in Chile, a middle income country in South America. The Neonatal Intensive Care Unit (NICU) consists of 25 beds, 8 of which are Intensive Care beds, 5 are Hybrid (for Intensive or Intermediate Care) and 12 are Intermediate Care beds. A total of 15 neonatologists, 50 bedside nurses and 47 nurse assistants influence this care process. The NICU coverage rate for bedside nurses is 1 per 3 patients and for nurse assistants 1 per 2 patients. There are 2 Neonatology attendings in house and 2 additional Neonatology Coordinator attendings that provide continuity of care.

During FY 2017 the NICU had 6,997 bed days and occupancy of 76%. A total of 1.5% (n=55) of admitted infants were < 1500g and/or < 32 weeks gestational age at birth. In this group of premature infants, from January 2016 to June 2018 the average LOS was 59.1 days and the average weight for gestational age delta z score upon discharge was -0.42. Premature infants are at increased risk of acquiring CLABSIs related to a longer duration of hospitalization, increased need for central lines for nutrition and intrinsic immunodeficiency.

Problem description/rationale

During FY 2015 a multidisciplinary team within the NICU developed insertion and maintenance central line checklists, and kept close surveillance of protocol adherence in all patients with central lines. During FY 2016 the NICU reached and maintained a CLABSI rate of zero. From June 2017, the CLABSI rate in the NICU increased from 0 to 17.9 per 1.000 line days (includes umbilical, central and peripherally inserted central lines). During the following months the rate increased to 22 per 1.000 line days. We performed a Fishbone diagram and acknowledged the following main topics: (1) increased nº of infants <1500g, (2) hybrid bed infrastructure suboptimal for intensive care, (3) decrease in checklist surveillance and CLABSI team audit meetings, and (4) increase in census. The average census in the Intensive care beds for the first semester of FY 2017 was 98%, but from July 2017 it increased up to 138%, which implied using Hybrid beds for Intensive care.

In the literature, an infant with a CLABSI may increase their LOS at least 10 days and increase the cost of their hospitalization by USD 50.000. Additionally, premature infants that present with a CLABSI pose a higher risk of bronchopulmonary dysplasia, retinopathy of prematurity, necrotizing enterocolitis, short gut syndrome, malnutrition and death. In alignment with our Institutional goal, we aimed to decrease our CLABSI rate back to zero, as in FY 2016.

Aim

To reduce CLABSI rates in hospitalized infants in the NICU from 14 to 2 per 1.000 line days by February 28, 2018 and to 0 per 1.000 line days by May 30, 2018. CLABSI was defined per CDC recommendations.

Drivers of change

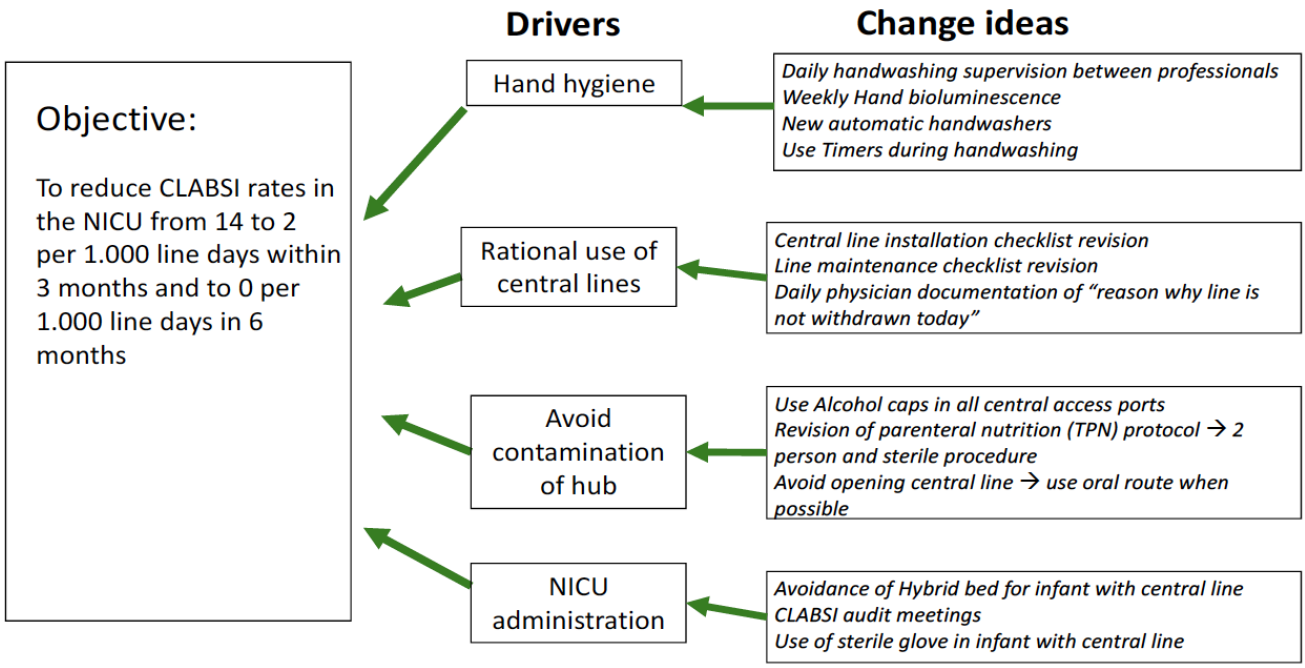

Interventions

- **PDSA nº 1 CLABSI Bundle**
  - **PDSA cycle 1a:** Development of Bundle and checklists
  - **PDSA cycle 1b-1e:** Bundle item applicability (handwashing surveillance, TPN administration checklist, central line installation and maintenance checklist, and documentation)
  - **PDSA cycle 1f:** Implementation of Bundle
- **PDSA nº 2 Physician central line Documentation**
  - **PDSA cycle 2a:** Phrase Development
  - **PDSA cycle 2b-2c:** Phrase incorporation and revision in daily note
  - **PDSA cycle 2d:** Phrase implementation
- **PDSA nº 3 Total parenteral nutrition (TPN) procedure**
  - **PDSA cycle 3a:** TPN updated procedure
  - **PDSA cycle 3b-3c:** TPN procedure simulation
  - **PDSA cycle 3d:** TPN procedure implementation
- **PDSA nº 4 Central line cap**
  - **PDSA cycle 4a:** Search for appropriate cap
  - **PDSA cycle 4b-4c:** Cap use simulation
  - **PDSA cycle 4d:** Cap implementation
- **PDSA nº 5 Timer for handwashing**
  - **PDSA cycle 5a:** Search for appropriate timer in compliance with local regulations
  - **PDSA cycle 5b:** Timer simulation use
  - **PDSA cycle 5c:** Timer implementation

Measures

Measure	Numerator	Denominator	Unit of measure	Test population	How was data obtained	Frequency of measurement	Data shared with team and senior leaders
OUTCOME							
CLABSI rate	Nº of hospitalized infants with CLABSI	Total nº of line days in infants with central lines	1000 line days	Infants in NICU	EMR	Monthly	Yes
PROCESS							
CLABSI Bundle compliance							
Handwashing	Nº workers hand hygiene according to guideline	Nº workers that were evaluated	%	Workers in NICU	Checklist	Daily	Yes
Central line installation	Nº infants with complete central line checklist	Nº infants with central line	%	Nurse/Physician	Checklist	Per procedure	Yes
Central line maintenance	Nº infants with complete maintenance checklist	Nº infants with central line	%	Nurse	Checklist	Daily	Yes
Central line documentation	Nº of notes with correct line documentation	Nº of notes reviewed	%	Physician	EMR	Weekly	Yes
TPN procedure	Nº TPN change per procedure	Nº TPN changes	%	Nurse	Checklist	Daily	Yes
Bioluminescence	Nº workers with bioluminescence < 80 Ursl	Nº workers with bioluminescence	%	Workers	Nurse report	Weekly	Yes
BALANCING							
Weight Delta z score at discharge	Delta z score for weight at discharge in <1500g	-	z score	Infant	EMR	At discharge	Yes

Results

1. Outcome metric: CLABSI rate per month

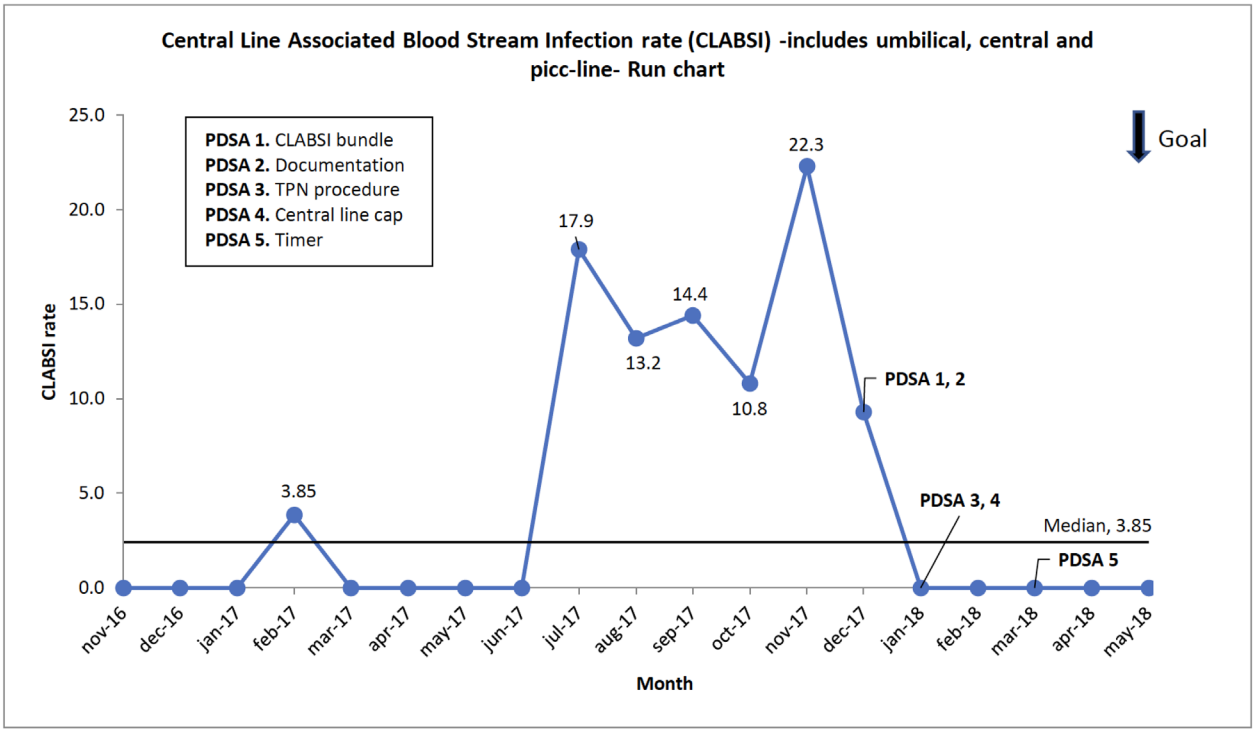

2. Process metric:

a. Bundle compliance

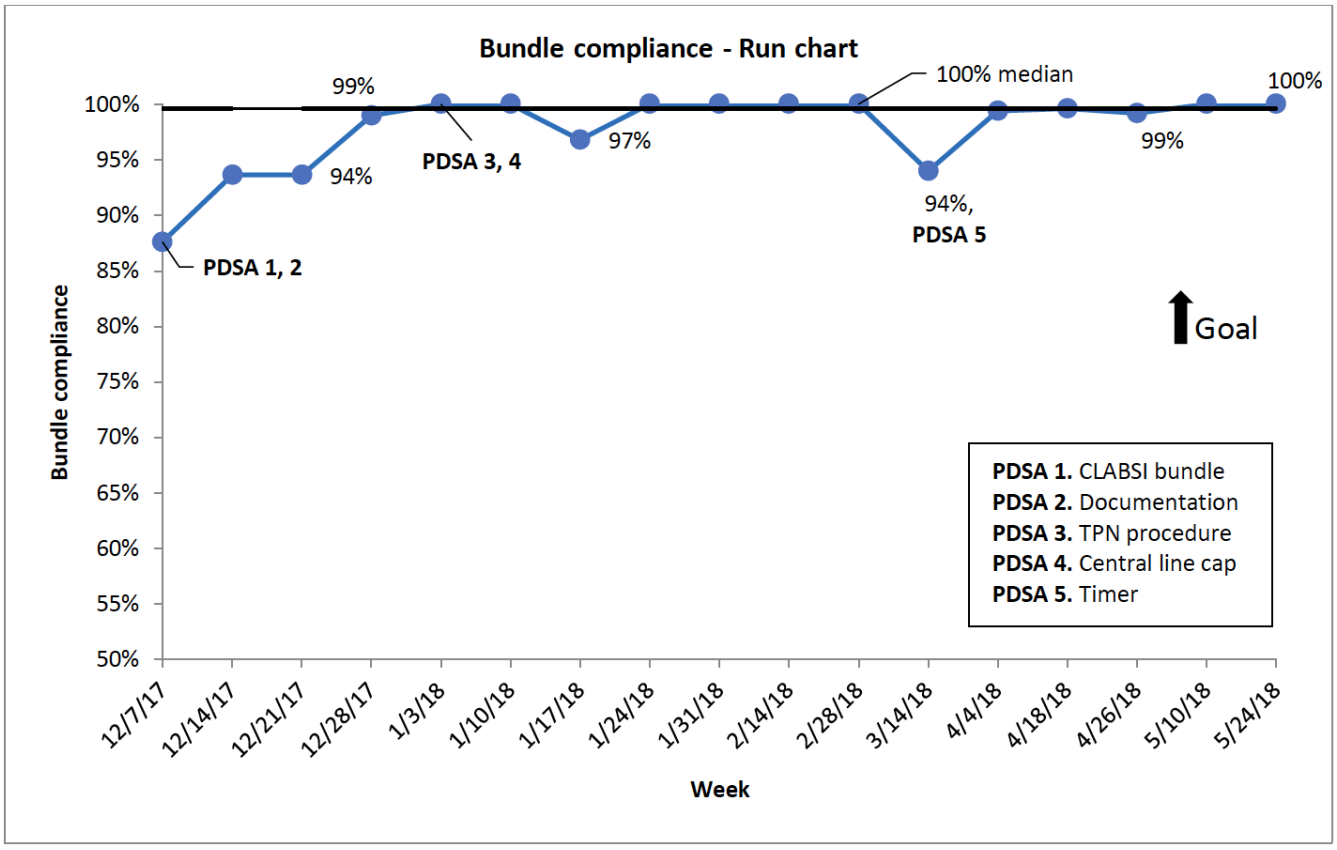

b. Bundle compliance per item

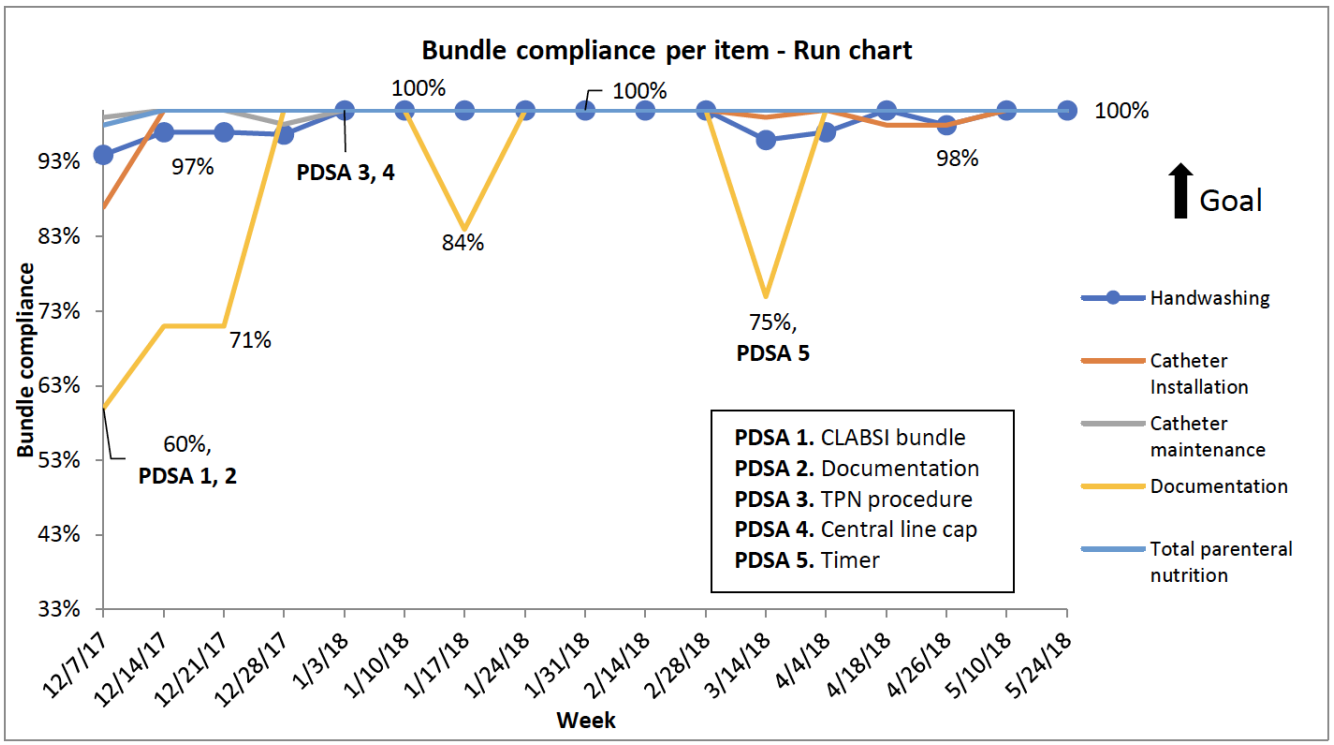

c. Hand Bioluminescence

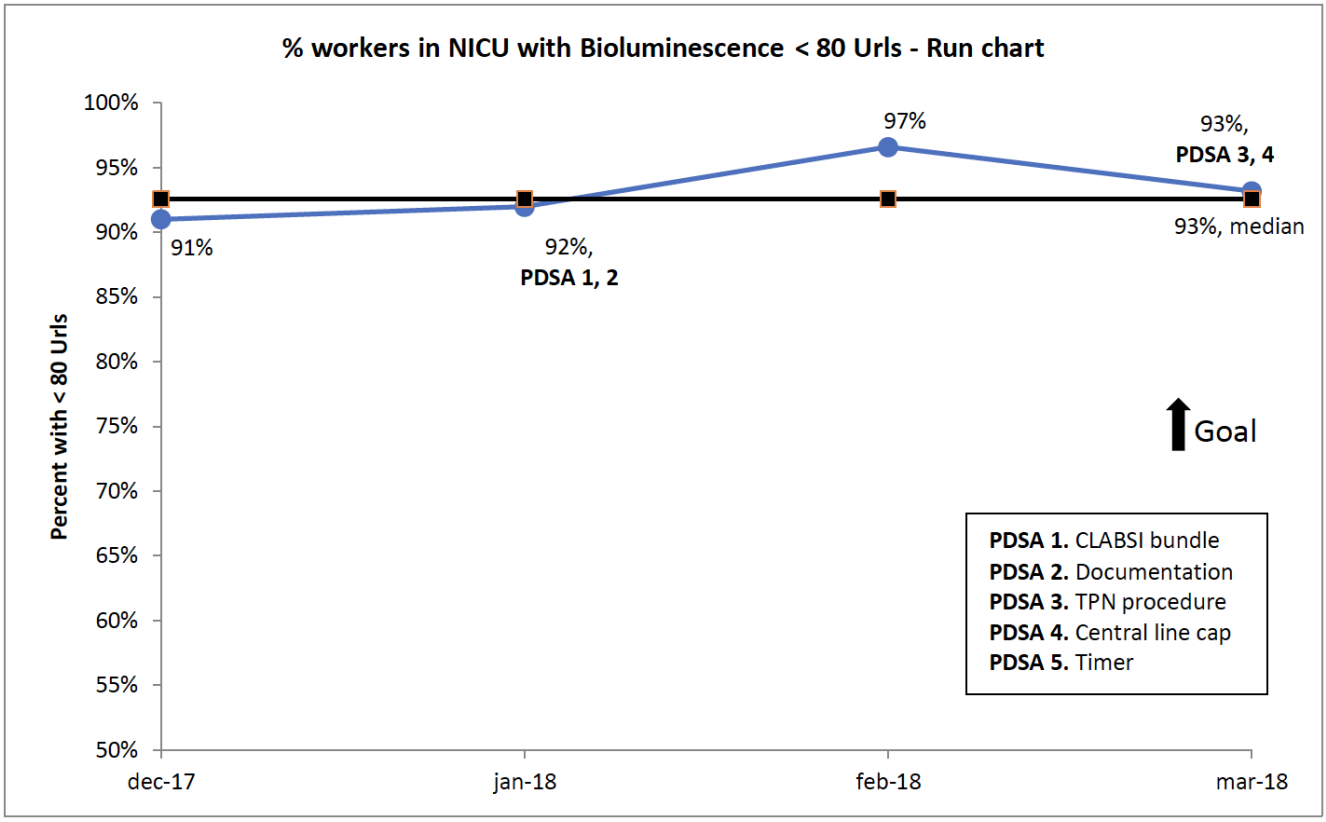

3. Balancing metric

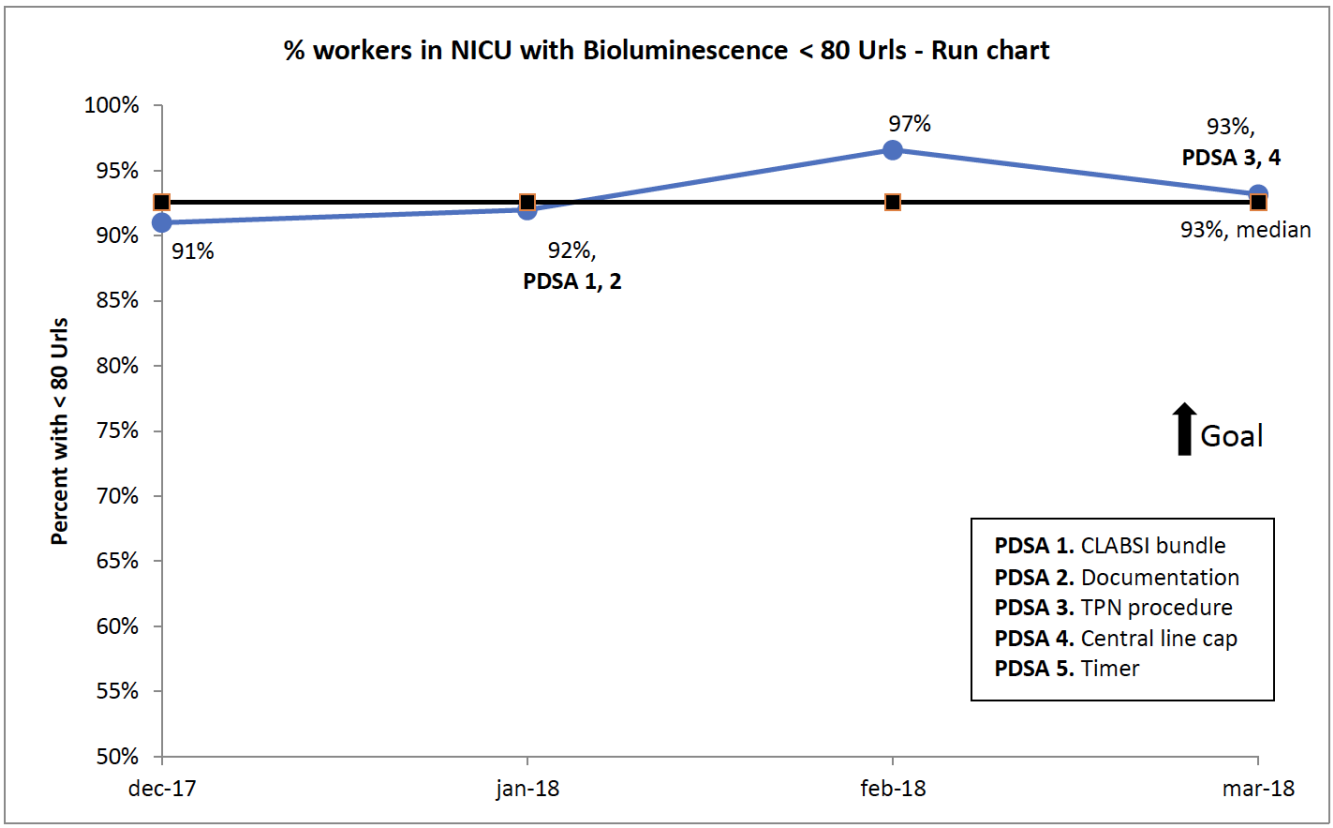

Discussion

Premature infants are prone to CLABSIs due to intrinsic factors. Nevertheless, CLABSIs are considered to be preventable. Quality Improvement methodology and bundle implementation has demonstrated success in reducing the rate of CLABSIs in the NICU.

In this project, we implemented a bundle that consisted of: (1) hand hygiene protocol supervision, (2) central line installation procedure, (3) central line maintenance procedure, (4) central line documentation, and (5) a sterile 2 person TPN change procedure.

After 6 months of implementation, we obtained a bundle compliance greater than 95% and have maintained the effort. We have not had a CLABSI event in 165 days. Physician central line documentation needs further improvement and sustainability. Despite being more vigilant in removing central lines and the potential for increased extrauterine malnutrition, the delta z score for weight at discharge in infants <1500g did not decline. Our limitations include: a short time period of evaluation and a lower intensive care bed occupation during the bundle implementation time period. In order to sustain the gains, we are developing a Harm Prevention committee within the NICU and incorporate bundle compliance in our system.

Keywords

Central line-associated blood stream infections (CLABSI)
Premature infants
Infectious disease
Bundle
CLABSI bundle
Hand hygiene
Central line

Team acknowledgement

- Juan Carlos Muñoz MD, project physician leader, contributed in checklist development, physician documentation tracking, CLABSI audits, development and abstract revision.
- Beatriz Milet MD, project Improvement Advisor (IHI), contributed in quality improvement methodology, checklist revision, data analysis, CLABSI audits, development and abstract revision.
- Marcela Gómez RN, contributed in the development of new TPN protocol, checklist development and supervision, participated in CLABSI audits and abstract revision.
- Antonieta Vicentelo RN, contributed in the development of new TPN protocol, checklist development and supervision, participated in CLABSI audits and abstract revision.
- Marta Contreras RN, contributed in the development of central line and TPN protocols, CLABSI audits, performs weekly bioluminescence and abstract revision.
- Marissa Garrido RN, project nurse leader, contributed in the development and revision of checklists, supervision of line maintenance, TPN changes, CLABSI audits and abstract revision.
- Carolina Avila RN, project nurse leader, contributed in the development and revision of checklists, CLABSI audits and abstract revision.
- Pablo Gaete MD, contributed in the development of central line and TPN protocols, CLABSI audits and abstract revision.
- Marcial Osorio MD, NICU Director and stakeholder, contributed in CLABSI audits and abstract revision.

Abstract 32.

Seis pacientes con trombosis de seno venoso en tratamiento con Dabigatran

Dra. Marianella Hernández, Dra. Patricia Araneda, Dr. Sergio Illanes.
Departamento de Neurología y Psiquiatría, Clínica Alemana de Santiago

Presentado en 16th Annual Meeting Neurocritical Care Society, 25-28 septiembre de 2018, Miami, Estados Unidos.

La trombosis de seno venosos cerebral (TSV) tiene una incidencia de 2-5 casos por millón, con un aproximado de 15% de muerte o dependencia, afectando frecuentemente a los adultos jóvenes con edad media de 35 años, siendo más común en mujeres, y siendo estructuralmente más afectados el Seno Sagital Superior y Transverso.

Actualmente el único manejo aprobado que existe es la heparina e inhibidores de vitamina K.

Objetivo: evaluar la efectividad y seguridad de Dabigatran en pacientes con trombosis de seno venoso.

Materiales y métodos: estudio observacional, descriptivo y transversal. Se consideraron 6 pacientes con TSV que fueron tratados con Dabigatran.

Resultados: durante el seguimiento de hasta 8 años, no hubo recurrencia de trombosis ni complicaciones asociadas al tratamiento.

Discusión: en nuestra serie observamos que Dabigatran fue útil para el manejo de TSV en aquellos pacientes que no pudieron utilizar inhibidores de vitamina K por diferentes motivos, sin haber recurrencia de eventos trombóticos, ni complicaciones durante su seguimiento, incluso en pacientes con trombofilia diagnosticada.

Conclusión: Dabigatran sería efectivo y seguro para el manejo de TSV en nuestra cohorte. Se encuentra en curso un estudio clínico que busca probar la eficacia y seguridad en estos pacientes. Este será, probablemente, el próximo paso en el tratamiento de nuestros pacientes, ya que es más cómodo, seguro y fácil de utilizar.

Abstract 33.

Experiencia de atención odontológica bajo anestesia general en pacientes odontopediátricos con y sin necesidades especiales en salud. Estudio retrospectivo.

Ximena Muñoz[1], María Consuelo Fresno[1-2], Javier Martin[2].

[1]Servicio de Odontología Clínica Alemana de Santiago, Chile.
[2]Facultad de Odontología Universidad de Chile. Santiago, Chile.

Presentado en XIX Congreso Asociación Latinoamericana ODP, 18 de octubre de 2018, Montevideo, Uruguay.

Resumen

Objetivos: Determinar características de edad, sexo, tipo de procedimientos en relación con diagnóstico de ingreso y existencia de patología médica de base (PMB) en pacientes odontológicos tratados bajo anestesia general. Estudio de cohorte retrospectivo.

Metodología: Se analizaron 92 pacientes menores de 14 años tratados odontológicamente bajo anestesia general en una sesión, desde 2013 a 2018 en el Servicio de Odontología de la Clínica Alemana de Santiago, Chile. Se registró género, edad al pabellón, diagnóstico de ingreso, presencia o no de PMB y tratamiento realizado (simple o complejo).

El análisis estadístico se realizó utilizando software IBM® SPSS® Statistics v. 25, pruebas de Chi2 y Z de proporciones para comparar los pacientes con y sin PMB.

Resultados: La edad varió entre 1 año 10 meses y 13 años 4 meses, predominando hombres (60,9%, n=56) sobre mujeres (39,1%, n=36) ($p<0,05$). 23,9% presentaban PMB y 72,8% fueron tratamientos complejos. El principal diagnóstico fue CTI Severa con 63%.

Se observó que CTI severa es mayor en pacientes sin PMB (72,9% vs 31,8%), la consulta por caries múltiples es mayor en los pacientes con PMB (22,7% vs 5,7%) ($p<0,05$).

Conclusiones: La atención odontológica bajo anestesia general es una alternativa segura y efectiva para tratar a pacientes no colaboradores o que presentan necesidades especiales en salud.

Palabras clave: anestesia general, caries, odontopediatría.

Abstract 34.

Risk for central metastasis on papillary thyroid cancer patients with suspicious lateral lymph nodes and non suspicious central LN on preoperative staging ultrasound (US)

Ingrid Plass[1], Hernán Tala[2], Eleonora Horvath[2], Paulina González[2], Juan Pablo Niedmann[2], Carolina Whittle[2], Jeannie Slater[2], Felipe Capdeville[2], Arturo Madrid[2], Hugo Rojas[2], Ricardo Rossi[2], Fabio Valdés[2]

[1]Head and Neck Surgery, Clinica Alemana de Santiago, Santiago, RM, Chile
[2]Thyroid Center, Clinica Alemana de Santiago, Santiago, Chile

Presentado en 88th Annual Meeting of the American Thyroid Association, 3 al 7 de octubre 2018, Washington D.C., Estados Unidos.

We aim to establish the risk for clinically relevant central lymph node metastasis (CRCM) on papillary thyroid cancer (PTC) patients with suspicious lateral lymph nodes on preoperative ultrasound (SLN) and non suspicious lymph nodes on the central compartment. Retrospective review of PTC patients with a preoperative staging US showing SLN, who underwent lymph node resection at our institution, between 2013 and 2017. We defined as suspicious lymph node, central or lateral, those with micro/coarse calcifications, cystic areas, hyperechoic spots, and hypervascularization with capsular vessels.

We studied the risk for CRCM >2mm and ǂ5mm on pathology and categorized our patients according to the central neck preoperative staging US on suspicious, uncertain and normal. We defined as "uncertain" those prominent central lymph nodes associated with Hashimoto's Thyroiditis, peri-istmic/infrathryoid, hypoechoic and with no hilum; or those accompanying an identified PTC that do not have typical suspicious characteristics.

Finally, we studied other preoperative variables in order to assess their impact on the risk for CRCM. We reviewed 77 patients (65% women, median age 39 years). CRCM >2mm were present on 74% (57/77), whereas CRCM ǂ5mm, on 45% (35/77). According to the evaluation of the central compartment on US, 36% (28/77) had a normal sonographic pattern: of them, 68% (19/28) had CRCM >2mm and 32% (9/28) had CRCM ǂ5mm. An uncertain central US pattern was established on 21% (16/ 77): of them, 69% (11/16) had CRCM >2mm and 50% (8/16) CRCM ǂ5mm. On the assessment of preoperative variables, presenting ǂ3 SLN was significantly associated to an increased risk for CRCM >2mm (68% vs 97%, p = 0.002) and for CRCM ǂ5mm (37% vs 68%, p = 0.014). A significant risk for CRCM exists on PTC with SLN on the staging preoperative US, which is maintained even for patients with normal central sonographic patterns. The risk increases for patients with uncertain central lymph nodes on the US. Larger number of SLN on US is significantly associated to a greater risk for central metastases. This information should be used to consider central lymph node dissection when SLN are detected on staging US, even in the absence of suspicious central LN.

Abstract 35.

Pentoxyphylline inhibits M1 polarization and favors M2 of murine macrophages treated with TLR4 agonist.

María Cecilia Montero[1] MVD MSc, Julia Guerrero[1,2] MD PhD

[1] Laboratorio de Inmunomodulación Neuro- Endocrina del Programa de Fisiología, Instituto de Ciencias Biomédicas (ICBM), Facultad de Medicina Universidad de Chile.
[2] Unidad de Cuidados Intensivos, Clínica Alemana de Santiago

Presentado en Congreso Europeo de Medicina Intensiva (ESICM), 20 al 24 de octubre, París, Francia.

Introduction

Pentoxyphylline (PTX) is a phosphodiesterase inhibitor that increases intracellular cAMP. Recently, PTX has been recognized as a pharmacological modulator of inflammation that may improve outcomes in septic patients [(1)]. In neonatal sepsis, the use of PTX as an adjunct to antibiotics therapy decreased all-cause mortality and the length of hospital stays, without significant adverse effects [(2)]. Authors had proposed its effect may be mediated by adenosine-dependent pathways for polymorphonuclear leukocytes and T cells [(3)]. Results of studies in whole new born umbilical blood showed that PTX inhibited the inflammatory cytokine response induced by Toll-like receptors (TLR) agonists, TLR4, TLR7 and TLR8 [(4)]. Considering that peripheral blood macrophages can reprogram their phenotype and orchestrate the inflammatory response, we tested if PTX modifies inflammatory cytokines profile in response to a TLR-4 agonist in a macrophage cell line.

Objetive: To assess if PTX modulates macrophage TLR4-dependent polarization in vitro.

Methods: Murine macrophages (Raw 264.7 cells) were cultured in Dulbecco's Modified Eagle's Medium (DMEM) (control), or in the presence of lipopolysaccharide (LPS, Sigma - Aldrich Chemie®, Germany) 25ng/mL, LPS + PTX (dose-response curve; Sigma-Aldrich Chemie®, Germany) or PTX alone. We analyzed cell viability by trypan blue exclusion assay and the time-course of changes in TNF-alpha and IL-10 mRNA content (as surrogate markers of M1 or M2 polarization, respectively) in the presence or absence of LPS, PTX or LPS plus PTX by real-time qPCR.

Results: PTX (100-250-500 and 1000µg/ml by 1-1.5 or 2h) had no effect on cell viability or TNF-alpha mRNA abundance. LPS induced TNF-alpha mRNA (3 times of control level; n= 4, p<0,05) and PTX inhibited TNF-alpha mRNA induced by LPS (p<0,05). The inhibitory effect of PTX on LPS-dependent TNF-alpha mRNA induction was greater with 250 µg /ml and over 1h of exposition. Interestingly, after 1.5 h of exposure, PTX+ LPS significantly increased the cellular content of IL-10 mRNA.

Conclusions: PTX modulates macrophage inflammatory cytokines response induced by a TLR-4 agonist. We postulate that PTX modifies the polarization profile of macrophages (M1 to M2). In the context of TLR4 activation, the increase of cAMP induced by PTX may activates PKA, stabilize the IκB inhibitor and suppress NF-κB nuclear translocation. Besides, cAMP-PKA-dependent CREB phosphorylation may explain the induction of IL-10 mRNA at a transcriptional level.

References

1. *Staubach K-H, Schroder J, Stuber F et al. Arch Surg 1998.*
2. *Pammi M, Haque KN. Cochrane Database Syst Rev 2015.*
3. *Kreth S, Ledderose C, Luchting B, et al Shock 2010.*
4. *Speer EM, Dowling DJ, Ozog LS et al. Pediatric Research 2017.*

GRANT ACKNOWLEDGMENT: this study was financed with own resources.

Abstract 36.

Extracorporeal life support in critical ill immunocompromised adult patients

René López, Rodrigo Pérez, Jerónimo Graf.

Unidad de Cuidados Intensivos, Departamento de Paciente Crítico, Clínica Alemana de Santiago
Facultad de Medicina, Clínica Alemana – Universidad del Desarrollo
Santiago, Chile

Presentado en 31st Annual Congress ESICM Lives 2018, 20 al 24 de octubre, París, Francia.

Acute respiratory failure (ARF) is the first reason for admission to ICU in immunocompromised patients and although survival improved markedly improved in recent years, when need invasive mechanical ventilation remain having significant mortality. Extracorporeal life support (ECLS) depicts one of the ultimate therapies in intensive care and may possibly be beneficial in patients with acute respiratory distress syndrome (ARDS) in general ICU population. Nevertheless, the immunocompromised state has been described as most common relative contraindication to ECLS [1].

Recently, novel data has emerged about ECLS in patients with hematological malignancies [2] and AIDS-related pneumocystis jirovecii [3]. However,limited data is available about the type of ECLS according if the purpose was oxygenation or extracorporeal CO2 removal (ECCO2R).

Objectives

Describe the cohort immunocompromised patients on ECLS referral to immunocompetent patients.

Methods

Analysis of cohort of patients supported with respiratory ECLS, with focus on immune status and type of ECLS. Respiratory ECLS was delivered as veno-venous extracorporeal membrane oxygenation (VV-ECMO) if catastrophic respiratory failure, or as extracorporeal CO2 removal (ECCO2R) if ventilations is impaired and could not be optimized keeping protective ventilation. Immunocompetent patients with influenza A H1N1 (H1N1) related ARDS supported with ECLS and immunocompromised patients supported with ECLS.

When was possible, mortality proportions were compared with chi-square.

Results

We identified 45 patients with respiratory support, twelve of them (27%) were immunocompromised: hematology malignancies (5), AIDS (1), pulse of steroids and other drugs [6]. On other hand, 15 patients were positive to H1N1 and the group of patients non-immunocompromised (without H1N1) were 18 patients (60%). Demographic and ECLS support details of immunocompromised patients in Table 1 and Table 2.

Table 1.

ID	Gender	Age (years)	Diagnostic	ECLS type	Time run (days)	Outcome
1	Female	35	Myeloid Leukemia	AV ECCO2R	9	Alive
2	Male	53	Steroids + Methotrexate	AV ECCO2R	80	Dead
3	Female	27	Steroids + Cirrhosis	AV ECCO2R	21	Alive
4	Male	40	Lymphoma B	AV ECCO2R	2	Dead
5	Female	29	Myeloid Leukemia	AV ECCO2R	2	Dead
6	Female	58	Steroids + Mycophenolate	VV ECCO2R	11	Dead

[Demographic and ECCO2R data of immunocompromised patients]

Table 2.

N	Gender	Age (years)	Diagnostic	ECLS type	Time run (days)	Outcome
1	Male	70	Steroids	VV ECMO	10	Dead
2	Male	52	Neutropenia	VV ECMO	8	Alive
3	Male	34	AIDS	VV ECMO	24	Alive
4	Male	66	Steroids	VV ECMO	18	Alive
5	Male	42	Plasm Cells Leukemia	VV ECMO	11	Alive
6	Female	54	Steroids	VV ECMO	6	Alive

[Demographic and VV ECMO data of immunocompromised patients]

Four patients were diagnosed with pneumocystis pneumonia, two of them died.

We found difference on inhospital mortality only between patients immunocomp etent H1N1 versus immunocompetent non-H1N1 on ECLS, 58% vs 20% respectively (p=0.028). Inhospital mortality according to ECLS and ECLS types are showed in Figure 1.

Conclusions

A similar survival b etween immunocompromised and non-immunocompromised patients supported with ECLS was watched. Probably, with more data, immunocompromised state as contraindication to ECLS could be reconsidered. More data about immunocompromised patients on ECLS is required.

Figure 1.

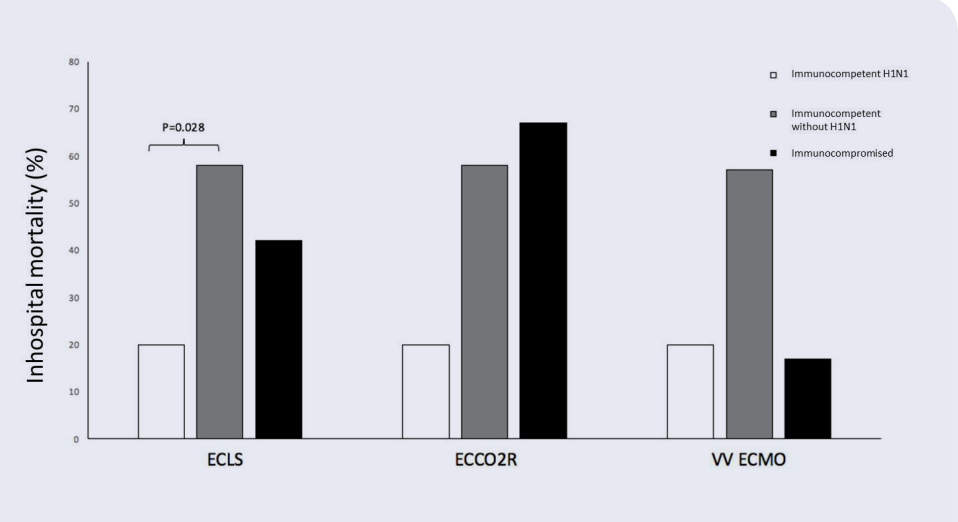

References

1. *Bohman JK, Vo gt MN, Hyder JA. Heart Lung. 2016; 45:227-231.*
2. *Wohlfarth P, Ullrich R, Staudinger T, et al. Crit Care 2014; doi: 10. 1186/cc13701.*
3. *Ali HS, Hassan IF, George S. BMC Pulm Med 2016; doi: 10.1186/s12890-016-02 14-4.*

Grant acknowledgment
None.

Abstract 37.

VE/VCO_2 slope is increased in patients who fail the spontaneous breathing trial

René López MD[1], Rodrigo Pérez RRT[1], Iván Caviedes MD[1], Jerónimo Graf MD[1]

Departamento de Paciente Crítico, Clínica Alemana de Santiago,
Facultad de Medicina Clínica Alemana - Universidad del Desarrollo, Santiago, Chile.

Presentado en 31st Annual Congress ESICM Lives 2018, 20 al 24 de octubre, París, Francia.

Comentario

El trabajo de investigación ha demostrado la superioridad del índice VE/VCO2 (ventilación necesaria para eliminar 1 litro de CO2), sobre el parámetro de mayor uso en el retiro del ventilador mecánico (volumen corriente/frecuencia).

Rationale

An increased respiratory rate (f) associated with a tidal volume (TV) reduction, is observed in patients who fails the spontaneous breathing trial (SBT) in weaning of mechanical ventilatory support.

It is measured with the rapid shallow breathing index (f/TV). This inefficient pattern is associated with a rising PaCO2 despite constant minute ventilation (VE).
Direct assessment of ventilatory inefficiency along SBT has not been reported.
As parallel, in stress conditions as cardiopulmonary exercise test, ventilatory inefficiency is assessed with the VE to CO2 production ratio (VE/VCO2), or its slope.

Hypothesis

Ventilatory inefficiency measured as VE/VCO2 relation, is increased in patients whom fails the T-piece SBT.

Objective

Determine if Ventilatory inefficiency, measured as VE/VCO2 relation, is increased in patients
whom fails the weaning of mechanical ventilatoy support.

Methods

1. One-hour SBT was prospectively evaluated in 77 patients.
   A CO2/flow sensor was installed between the endotracheal tube and T-piece.
2. Follow variables were recorded from a volumetric capnography monitor.
   f, TV, VE and VCO2 at 1, 15, 30, 45 and 60 minutes were measured.
3. f/VT and VE/VCO2 relations were calculated.
4. Trial failure was defined according to standard criteria.

f: respiratory rate
TV: tidal volume
SBT: single breath trial
VE: minute volume
VCO2: CO2 production

Demographics

Male N (%)	46 (59,7)
Age in years (SD)	62 (17)
APACHE II (SD)	15 (2)
Days on invasive ventilation (SD)	5 (0.5)
Diagnostic N (%)	
Surgical	16 (20.8)
Pneumonia	7 (9.1)
Sepsis	15 (19.5)
Trauma	6 (7.8)
Neurological	8 (10.4)
COPD	1 (1.3)
Others	23 (30)
Outcome, SBT failure N (%)	23 (30)

STATISTICS: Descriptive.
Means and SD calculation.
StudentsT test.
AUC [CI] of the ROC curves calculation.

Results

Twenty-three patients (30%) failed the SBT.
Variables from SBT failure compared to success patients were the following:
f/VT at 1 min: 79 ± 10 vs 52 ± 3 (p=0.03), and f/VT at 60 min: 91 ± 10 vs 53 ± 3 (p=0.01). VE/VCO2 at 1 min: 44 ± 3 vs 41 ± 2 (p=0.36), and VE/VCO2 at 60 min: 56 ± 6 vs 29 ± 3 (p<0.001).

The AUC [CI] of the ROC curves were 0.66 [0.52 - 0.80], 0.71 [0.57 - 0.86], and 0.81 [0.70 - 0.93] for f/VT at 1min, f/VT at 60 min, and VE/VCO2 respectively.

	1 minute Failure/success	p value	60 minutes Failure/success	p value
f/TV	79 ± 10 / 52 ± 3	0.03	91 ± 10 / 53 ± 3	<0.01
VE/VCO2	44 ± 3 / 41 ± 2	0.36	56 ± 6 / 29 ± 3	<0.001

Comparison between f/TV and VE/VCO2, in patients who failed or succeed to the SBT at 1 and 60 minutes

f: respiratory rate
TV: tidal volume
SBT: single breath trial
VE: minute volume
VCO2: CO2 production

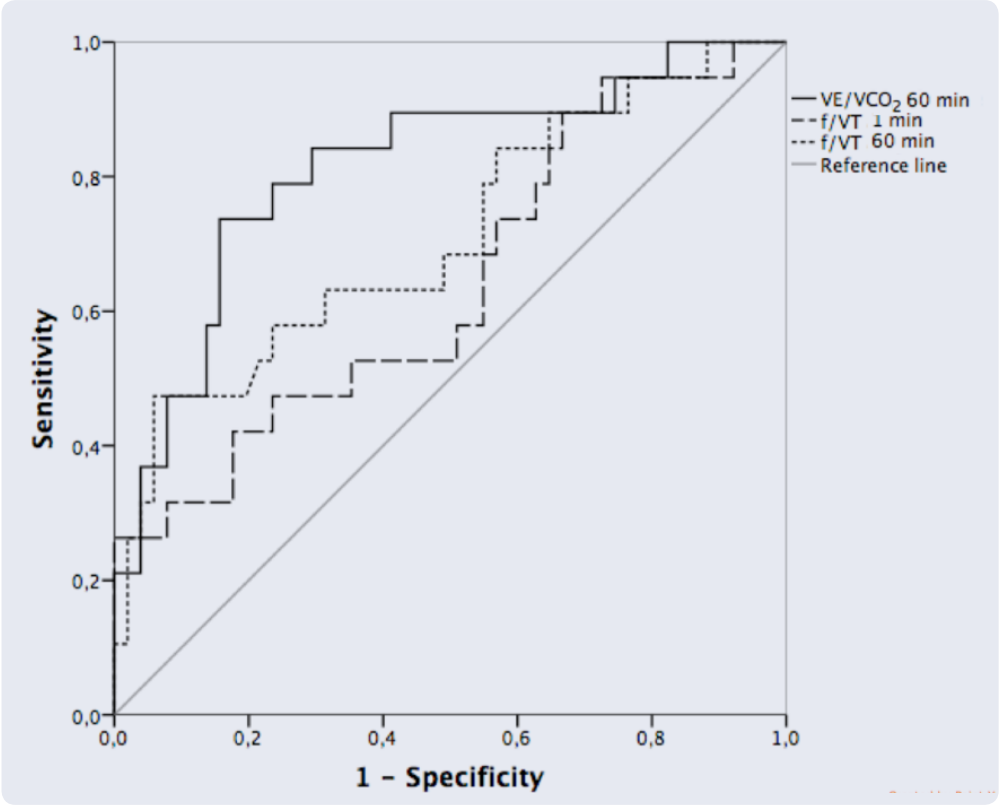

Conclusion

Our data suggest that Ventilatory inefficiency represented by an increased VE/VCO2 along the SBT, is a physiological trait of patients in weaning of mechanical ventilatory support.

Abstract 38.

South American scrub typhus: first case series from continental Chile

Thomas Weitzel[1], Constanza Martínez-Valdebenito[2], Gerardo Acosta-Jamett[3], Ju Jiang[4], María Pilar Gambra[5], Teresa Bidart[5], Miguel Lagos[6], Allen L. Richards[4], Katia Abarca[2].

[1]Clínica Alemana, Facultad de Medicina Clinica Alemana, Universidad del Desarrollo, Santiago, Chile; [2]Departamento de Enfermedades Infecciosas e Inmunología Pediátricas, Facultad de Medicina, Pontificia Universidad Católica de Chile, Santiago, Chile; [3]Instituto de Medicina Preventiva Veterinaria y Programa de Investigación Aplicada en Fauna Silvestre, Facultad de Ciencias Veterinarias, Universidad Austral, Valdivia, Chile; [4]Viral and Rickettsial Diseases Department, Naval Medical Research Center, Silver Spring, MD, USA; [5]Unidad de Infectología, Clínica Santa María, Santiago, Chile; [6]Hospital Los Angeles, Los Angeles, Chile.

Presentado en Congreso de Medicina Tropical, 28 de octubre – 1 noviembre, Nueva Orleans, Estados Unidos.

Scrub typhus is a neglected zoonotic disease endemic to the Asian-Pacific region and caused by *Orientia tsutsugamushi*. Until 2006, this potentially life-threatening rickettsiosis had never been detected outside these geographical limits; however, since then, patients reported from the Chiloé Island in Chile (n=3) and Dubai (n=1) suggest the emergence of the disease further afield. Here we report the first autochthonous scrub typhus cases from continental territories of Chile.

From 2016 to 2018 we detected a total of 9 scrub typhus cases acquired on mainland Chile, 7 male, with a median age of 28 years (range 21-69). All occurred during the summer months (Feb.-March) and were associated to outdoor activities; 7 were travel-associated and diagnosed on return to Santiago.

Infections were acquired in 3 different regions (Biobío, Los Lagos, and Aysén), ranging over a distance of 1,930 km (38°03'S to 47°47'S). Clinically, all presented with fever, maculopapular rash, eschar, and headache; other symptoms included myalgia, night sweats, and regional lymphadenopathy; 8 patients were hospitalized. Frequent lab abnormalities were elevated CRP and transaminases, thrombocytopenia, and leukopenia. All cases were confirmed by qPCR (*rrs*), PCR and sequencing (*rrs* and 47-kDa gene) using eschar material. Commercial serological tests for IgG (IFT, ELISA) and IgM (ELISA) using O. *tsutsugamushi* antigens were positive in 5/5 patients, but showed low titers. After treatment with doxycycline (n=7) or azithromycin (n=1), patients recovered rapidly; 1 patient recuperated without specific treatment.

This case series presents the first evidence of endemic South American scrub typhus in continental Chile. Our preliminary molecular analysis suggests that South American scrub typhus is caused by a distinct *Orientia* sp., which might explain the low *seroreactivity* against O. *tsutsugamushi* antigens. Vectors and possible zoonotic reservoirs are subject to ongoing studies. Our findings confirm the emergence of this important rickettsial infection and have significant impact on our understanding of the global epidemiology of the disease.

Abstract 39.

Imaging study of pulmonary vein stenosis

Julia Alegria MD, Claudio Silva MD,
Guillermo Aguilera MD,
Gerhard Franz Garrido.

Presentado en RSNA Meeting 2018, 25-30 noviembre, Chicago, Estados Unidos.
Digital Education Exhibit

Abstract

Obstruction of the pulmonary veins is a rare entity often difficult to diagnose since they are not evaluated on a regular basis when interpreting chest imaging studies. Its timely diagnosis is relevant since in advanced stages it has a poor prognosis. Currently, the most frequently encountered cause is secondary to radiofrequency ablation procedures performed to manage atrial fibrillation, but it can also occur due to pulmonary or mediastinal tumors, fibrosing mediastinitis, vein thrombosis or congenital defects. Regardless of the etiology, an obstruction of the pulmonary veins can translate into variable congestion of the segment dependent on the pulmonary parenchyma. High-grade obstructions might reach zones of pulmonary edema, pulmonary infarction and even massive hemoptysis. A review on relevant anatomy, main etiologies, and imaging findings of these pathologies will be provided in this article.

Abstract 40.

Intracranial Aneurysms Assessment: What the Radiologists Should Report

Tomas Bernstein, Nicolás Sanchez, Paulo Zuñiga Bustos.
Santiago, Chile

Presentado en RSNA Meeting 2018, 25-30 noviembre 2018, Chicago, Estados Unidos.
Digital Education Exhibit

TEACHING POINTS

Comprehend the classification of cerebral aneurysms
Describe typical and atypical findings of intracranial aneurysms in CT and MRI
Learn important treatment considerations

TABLE OF CONTENTS/OUTLINE

Definition and classification of cerebral aneurysms: saccular, fusiform, dissecting and blood blister like aneurysms
Typical and atypical clinical presentation and rupture risks factors
Imaging findings in CT and MRI
Learn how to report complex and atypical aneurysms
After treatment imaging considerations
Radiologic key points for avoiding pitfalls

Abstract 41.

Inter-observer agreement in the classification of perifissural nodules as lymphnodes on chest CT

Juan Carlos Díaz MD; Claudio Silva MD MSc; Javier Cacho MD; Julia Alegría MD; Cristóbal Ramos MD.

Radiology Department, Clínica Alemana de Santiago, Santiago, Chile
Facultad de Medicina, Clínica Alemana-Universidad del Desarrollo

Presentado en RSNA Meeting 2018,. Tuesday Nov 27, 2018, Chicago, Estados Unidos.

PURPOSE

Determine the inter-observer agreement of chest radiologists classifying perifissural nodules (PFN) as intrapulmonary lymphnodes on chest CT.

METHOD AND MATERIALS

IRB-approved retrospective study, who approved a waiver on informed consent. All chest CT performed during a four-month period (March through July 2016) were reviewed for inci-dental pulmonary nodules by a senior chest radiologist who sub-classified them into three categories (typical PFN – likely intrapulmonary lymph node, atypical PFN and non-PFN) by using criteria by de Hoop et al. 120 cases were selected, studies were anonymized and re-viewed by three other senior chest radiologists, who classified them using the same criteria, unaware of the patients' history. Inter-observer agreement was analyzed using Cohen's kappa coefficient. 95% CI were calculated and statistical significance was considered at $p<0.05$.

RESULTS

The global agreement measured by Cohen's Kappa was 0.603 (95% CI: 0.560 - 0.661). When categories were regrouped, Kappa value for classifying "typical PFN " compared to the re-maining categories ("atypical PFN" and "not PFN") was 0.728 (95% CI: 0.690 - 0.754), in good range of concordance according to Altman et al. When the "not PFN" category was consid-ered (grouping together the remaining categories), Kappa values dropped to 0.530 (95% CI 0.473 - 0.587), moderate concordance according to Altman et al.

CONCLUSION

Incidental pulmonary nodules are a frequent finding in routine chest CT and are followed according to guidelines. Some of these nodules represent intrapulmonary lymph nodes and should require no follow-up. Our results show that there is good interobserver agreement in the classification of PFN as "typical" intrapulmonary lymph nodes. However, classifying as "atypical" PFN has a higher degree of variability, which might hinder its widespread use.

CLINICAL RELEVANCE/APPLICATION

The category of intrapulmonary lymph node has been incorporated in some European inci-dental pulmonary nodule guidelines, and recently mentioned on the Fleischner Society guidelines. To our knowledge, there are no studies analyzing inter-observer agreement in classifying nodules as intrapulmonary lymph nodes. Our results show that there is good in-terobserver agreement in the classification of pulmonary nodules as typical PFN, therefore highly suggestive of intrapulmonary lymph nodes and amenable to support the incorporation of this category in future guidelines.

Normas Editoriales

CONTACTO CIENTIFICO

I. PREPARACION DE UN ARTICULO

Los autores deben preparar manuscritos de acuerdo con los requerimientos definidos por el Comité Internacional de Editores de Revistas Biomédicas (ICMJE), que pueden ser consultados en Ann Intern Med. 1997;126:36-47 o www.icmje.org. Los reportes de ensayos controlados y randomizados deben cumplir con la normativa de inscripción y diseño correspondiente, que puede ser consultado en Ann Intern Med. 2001;134:657-662.

El manuscrito debe estar escrito en letra Times New Roman, tamaño 12, a doble espacio y debe ordenarse de la siguiente manera (1) página del título (2) resumen, (3) lista alfabética de abreviaciones usadas al menos tres veces en el cuerpo del manuscrito y en resumen, figuras y tablas, (4) texto con encabezados apropiados y conclusiones, (5) agradecimientos, (6) referencias, (7) figuras (8) leyendas de las figuras (con lista alfabética de abreviaciones), y (9) tablas (con lista alfabética de abreviaciones).

El texto del manuscrito debe ser enumerado en forma consecutiva, incluyendo el nombre del primer autor y el texto debe contenerse en un archivo procesable por Word. Las tablas pueden ser hechas con el mismo programa Word, y ubicarlas al final del manuscrito. Los esquemas, gráficos y algoritmos pueden ser hechos y enviados en Word, PowerPoint o Adobe Illustrator. Las figuras deben ser guardadas como formato jpg, gif, o tiff a un mínimo de 300 dpi y no deben insertarse en el texto del manuscrito, sino que deben guardarse como archivo separado.

Página del título

Título: Formular un título que refleje el contenido del artículo.

Autores: Incluir apellidos y nombre, grado académico, departamento e institución a la que pertenece.

Financiamiento y conflictos de interés: indicar si existió financiamiento y ayuda material para la investigación o trabajo descrito en el manuscrito (ej. número de Grant, agencia financiante, a quiénes).

Reimpresiones y correspondencia: incluir nombres, dirección, e-mail del autor a quien se dirigirán estos requerimientos.

Resumen o Abstract

Abstract de 200 palabras y un resumen en términos sencillos ("plain language summary") de 50 palabras que describa el objetivo del estudio y su resultado principal.
Se debe organizar en un formato estructurado, con los siguientes encabezados: Objetivo, Pacientes y métodos, Resultados y Conclusión.

--Asegurar que la información en cada sección del resumen, está contenida en la correspondiente sección del texto.

--En la sección "Pacientes y métodos" del resumen y del texto, incluir las fechas completas que abarcó el estudio.

--Incluir el número de registro de Ensayo clínico, al final del resumen, si es el caso.

Texto

Los artículos originales deben considerar un máximo total de 2000 palabras, la introducción un máximo de 250 palabras y la discusión de 500.

No debe ser superior a 2000 palabras en el resto de los artículos.

En la introducción mencionar los antecedentes disponibles respecto del tema de estudio, establecer el objetivo de la investigación o revisión y plantear la hipótesis de trabajo.

--Abreviar un término sólo si es utilizado al menos tres veces en el texto y definirlo la primera vez que se menciona.

En la sección de pacientes (o materiales) y métodos describir las características del grupo de estudio o del caso clínico, los criterios de inclusión/exclusión, los equipos y/o fármacos utilizados, la probación del comité de ética local.

si corresponde, el consentimiento informado de los participantes y el tipo de análisis estadístico.

--Expresar medidas en Unidades convencionales, entregando el factor de conversión a Unidades del Sistema Internacional.

--Entregar valores exactos de p, incluso si no son significativos. Redondear valores de p a dos dígitos, si los primeros dos números después del decimal son ceros, entonces redondear a tres números. El menor valor de p a reportar es p<0.001 y el mayor p>0.99.

--Usar nombres genéricos para fármacos y equipos. Si piensa que es importante usar un nombre de producto, indique manufactura y lugar donde fue producido, entre paréntesis.

--Los símbolos genéticos aprobados, descripciones y equivalencias pueden encontrarse en www.genenames.org.

--Para mutaciones genéticas, ver sitio web HGVS (www.hgvs.org o http://www.hgvs.org/rec.html).

En la sección de resultados, describir los principales hallazgos de forma lógica, con especial mención a los datos relevantes que pueden estar contenidos en tablas o gráficos. Evite duplicar la información en tablas y gráficos.

En la sección de discusión, analizar los resultados en relación a la información previamente publicada y sus limitaciones, destacando los aspectos importantes del estudio que puedan concluirse en atención al diseño del estudio.

De acuerdo a la modalidad del manuscrito, el texto debe contener diferentes secciones:

--En los trabajos originales, debe incluir las secciones de: Introducción, Pacientes y métodos, Resultados y Discusión.

--En los casos clínicos, debe incluir las secciones de: Introducción, Descripción del caso y Discusión.

--En las revisiones, debe incluir las secciones de: Introducción y Desarrollo del tema.

Agradecimientos

El autor debe asegurar que se ha obtenido permiso de quienes se agradecerá.

Referencias

Los autores son responsables de la certeza de sus referencias y de su completa cita en el texto. No incluir más de 35 referencias, priorizando aquellas más relevantes. La cita de referencias, en el texto, figuras y tablas deben ser consecutivas como aparecen en el manuscrito, utilizando número superíndice.

En la lista de referencias, incluir apellidos e iniciales del nombre de todos los autores (si son más de 6, enumerar tres y agregar "et al"), el título, fuente (las abreviaciones de revistas están contenidas en el index medicus), año, volumen, número y rango de páginas.

--Para el estilo apropiado de referencias, consultar: American Medical Association Manual of Style: A Guide for Authors and Editors, 10th ed. New York, NY; Oxford University Press; 2007:39-79.

--Ejemplos.

Revistas (Impresas)

1. Rainier S, Thomas D, Tokarz D, et al. Myofibrillogenesis regulator 1 gene mutations cause paroxysmal dystonic choreoathetosis. Arch Neurol. 2004;61(7):1025-1029.

Revistas (Online)

2. Duchin JS. Can preparedness for biologic terrorism save us from pertussis? Arch Pediatr Adolesc Med. 2004;158(2):106-107. Available at http://archpedi.ama-assn.org/cgi/content/full/158/2/106. Accessed June 1, 2004.

3. Kitajima TS, Kawashima SA, Watanabe Y. The conserved kinetochore protein shugoshin protects centromeric cohesion during meiosis. Nature. 2004;427(6974):510-517. doi:10,1038/nature02312.

Capítulos

4. Bithell TC. Hereditary coagulation disorders. In: Lee GR, Bithell TC, Foerster J, Athens JW, Lukens JN, eds. Wintrobe's Clinical Hematology. Vol 2. 9th ed. Philadelphia, PA: Lea & Febiger; 1993:1422-1472.

Libros

5. Guyton AC. Textbook of Medical Physiology. 8th ed. Philadelphia, PA: WB Saunders Co; 1991:255-262.

Web

6. International Society for Infectious Diseases. ProMED-mail Web site. www.promedmail.org. Accessed April 29, 2004.

En caso de citar comunicaciones personales (orales o escritas) y datos no publicados previamente, citarlos entre paréntesis en el texto e incluir fecha. No anotar en las referencias y asegurar que se ha obtenido el permiso necesario. Evitarlos, si es posible.

Tablas

Numerar las tablas en forma consecutiva, en el orden de cita en el texto. Escribir a doble espacio, cada tabla en una página separada. Designar un título para cada tabla y definir todas las abreviaciones usadas en la tabla, en una nota al pie.

- Usar letras minúsculas superíndice (a-z) para las notas al pie de la tabla.
- No enviar tablas como imágenes.

Figuras

Se deben citar todas las figuras en el texto y numerarlas en el orden de aparición. En la leyenda de la figura, realizar la descripción correspondiente, en hoja aparte. Incluir definiciones de cualquier abreviación que aparezca en la figura, permisos y cita apropiada.

- Usar símbolos superíndice (*, #, †) para las notas al pie de la figura.
- Para microfotografías, especificar tinción y magnificación original.
- Para cualquier figura con un paciente reconocible, debe contar con el consentimiento del paciente.
- Las figuras obtenidas de una fuente sin derechos de autor requieren permiso de la fuente de publicación, o bien ocultar facciones que permitan su reconocimiento.

Permisos

El uso de gráficos, tablas y figuras previamente publicados no está permitido, excepto cuando existe permiso formal para ello del autor original o de la fuente de publicación. La falta en la entrega de los permisos apropiados retrasará la publicación o necesitará la omisión de una figura o tabla en la cual no se ha recibido el permiso.

II. Secciones y Contenidos

Sección	Abstract	Nº palabras	Ref.	Figuras y tablas
Alerta	250 palabras	2000	35	Máximo 3
Buenas Prácticas Clínicas	250 palabras	2000	35	Máximo 3
Casos Clínicos	250 palabras	2000	35	Máximo 3
Campañas	250 palabras	2000	35	Máximo 3
Controversias	250 palabras	2000	35	Máximo 3
Cursos y Congresos	250 palabras	2000	35	Máximo 3
Editorial	-------			
Etica Médica	250 palabras	2000	35	Máximo 3
Estado del Arte	250 palabras	2000	35	Máximo 3
Farmacología	250 palabras	2000	35	Máximo 3
Guías y Protocolos	250 palabras	2000	35	Máximo 3
Investigación	250 palabras	2000	35	Máximo 3
Lectura Crítica	250 palabras	2000	35	Máximo 3
Links - Videos	250 palabras	2000	35	Máximo 3
Medicina Traslacional	250 palabras	2000	35	Máximo 3
Noticias	250 palabras	2000	35	Máximo 3
Perlas	250 palabras	2000	35	Máximo 3
Publicaciones CAS-UDD Estructurado	250 palabras	2000	35	Máximo 3
Quiz	------	200		
Tips para publicar	250 palabras	2000	35	Máximo 3
Temas	250 palabras	2000	35	Máximo 3
Trabajos originales	200 + 50 plain language summary	2750	50	Máximo 3

III. Revision y Aceptación

Envío de revisiones

Reenvíe su artículo seguido con "R1" en caso de ser primera revisión o "R2" en caso de segundo análisis. Adjunte un breve comentario respondiendo a los alcances presentados por los revisores, una copia del texto con control de cambios y una copia con formato definitivo.

Recibirá un e-mail confirmando la recepción de los archivos corregidos.

Aceptación

Si su artículo es aceptado para publicación, éste debe ser editado en base a las normas dictadas en American Medical Association Manual of Style: A Guide for Authors and Editors, 10th ed. New York, NY; Oxford University Press; 2007:39-79). El autor principal recibirá una copia diagramada en formato pdf para su visto bueno previo a publicación.

IV. Monografías

El último número de cada volumen estará destinado a un tema monográfico que incluirá Editorial, Introducción y al menos 6 artículos originales o de referencia, más un capítulo de conclusiones.

V. Conflictos de Interés

Potenciales conflictos de interés de los autores deben ser explícitos en el documento enviado para publicación.

CLINICA Alemana®